Master in Bioengineering

Combining NAMs and Spectral Imaging with FISH for the analysis of the gastric micro-biogeography

A Master's dissertation

of

Helena Maria Silva Teixeira

Developed within the course of dissertation

Held in

FEUP

Supervisor: **Doctor Andreia S. Azevedo**

Co-supervisor: **Prof. Nuno F. Azevedo**

Chemical Engineering Department

June of 2019

Acknowledgements

First of all, I would like to express my sincerest gratitude to my supervisor Doctor Andreia Azevedo for providing me the opportunity to work on this project, for her constant advice, guidance, effort insight, inestimable support and critical revision of all my work. You were always there helping to move the obstacles off the way and was present since day one and from whom I have learned a lot.

Special thanks to my co-supervisor Professor Nuno Azevedo being always so kind and available to help me with any problems faced during this project, for the scientific guidance and support.

I would like to thank both laboratories, at Lepabe and at i3S, for having welcomed me since the beginning. I am grateful to I3S team, Maria and Paula for invaluable assistance with confocal microscope. To the laboratory assistants, Carla, Silvia and Paula, I really appreciate all the support that you gave me during this thesis and for all the technical problems you help me to solve.

To the people in laboratory E-101, thank you for the way you received me, for the excellent work environment and camaraderie, for the moments of relaxation experienced during the long periods of waiting for hybridizations. You make my days in the laboratory funnier and easier to work and provided me the really good moments of friendship and fun that I will never forget.

To Joana, Filipa, Claudia and Ana, my bioengineering companions, I am so lucky to have you as my best friends. Fortunately, during our journey we ended up joining and starting this amazing group. Our sisterhood keep us together no matter what challenge us.

I express my gratitude to all my hometown friends, specially to Manuel, Maria Inês, David, Ana, Inês and Tânia for bringing me when I was feeling down, and for all the good moments that have the privilege to share with us.

Finally, to my family, especially, my parents and sister, that always believed in my professional capacities, for supporting me in every way possible. Your support gave me the power to face any problems and warmed me up at any moment.

This work was financially supported by:

- Project UID/EQU/00511/2019 - Laboratory for Process Engineering, Environment, Biotechnology and Energy – LEPABE funded by national funds through FCT/MCTES (PIDDAC);

- Project POCI-01-0145-FEDER-030431 (CLASInVivo) and PTDC/DTP-PIC/4562/2014 (Coded-FISH), funded by FEDER funds through COMPETE2020 – Programa Operacional Competitividade e Internacionalização (POCI) and by national funds (PIDDAC) through FCT/MCTES.

Abstract

After the discovery of *Helicobacter pylori*, the stomach was no longer considered a sterile environment. Although *H. pylori* may be the most relevant, it is not the only local bacterial culprit to gastric diseases. Thus, the possible impact of the microbiota in gastric diseases need to be defined. To address this issue the Fluorescent *in situ* Hybridization (FISH) and Nucleic Acid Mimic (NAMs) such as Locked Nucleic Acid (LNA) and 2'-O-Methyl (2'OMe) have been applied to rapidly detect and localize gastric microbial cells. However, the number of microorganisms that can be discriminated by conventional FISH technique is usually limited to 3 targets. Hence, another new technology, called spectral imaging-FISH, is emerging. This advanced technique affords the opportunity to separate closely overlapping fluorochromes that would otherwise be unresolvable using conventional methodology. The combination of spectral imaging-FISH with NAMs probes will allow create a more straightforward procedure to study the composition and spatial organization of the microbiota directly in the stomach.

In a first stage, eight versions of the universal Eubacteria LNA/2'OMe probe (EUB338) were coupled with different fluorochromes (Alexa Fluor 405, Alexa Fluor 488, Alexa Fluor 514, ATTO 532, ATTO 550, Alexa Fluor 594, ATTO 633 and ATTO 655) to rank the bacteria and the fluorochromes and match the bacteria displaying weaker fluorescence intensity with the brightest fluorochromes and vice-versa. Furthermore, the FISH technique using an LNA/2'OMe probe coupled to 7 different fluorochromes was applied to the 5 mouse gastric bacterial species, to *H. pylori* and *Citrobacter freundii*. The results demonstrated that, using spectral imaging on Leica TCS SP5 Confocal, it was possible discriminate these 7 fluorochromes in a multiplex assay. Additionally, it was verified that input into the mixture of mouse gastric bacterial species, *C. freundii* and *H. pylori*, has correlated with output after image analysis, thereby establishing biological proof of principle of spectral imaging-FISH.

Furthermore, species-specific LNA/2'OMe probes were designed for *C. freundii, Muribaculum intestinale and Faecalibaculum rodentium,* whereas for *H. pylori*, *Lactobacillus* sp., *Bacteroides* sp. and Clostridiales sequences available on literature were re-evaluated. These probes have high specificity and sensitivity, and a melting temperature of approximately 77.5ºC.

Together, the results confirm the accuracy of Spectral Imaging–FISH and establish as proof of the principle using mouse gastric bacterial species. This method has demonstrated an extraordinary ability to distinguish fluorochromes with highly overlapping emission spectra in a single linear unmixing algorithm.

Keywords: FISH, Gastric Microbiota, LNA/2'OMe, NAMs, Spectral Imaging

Resumo

Após a descoberta do *Helicobacter pylori*, o estômago deixou de ser considerado um ambiente estéril. Embora o *H. pylori* seja considerado o microrganismo mais relevante, não é a única bactéria responsável pelas doenças gástricas. Assim, o possível impacto da microbiota nas doenças gástricas necessita de ser definido. A técnina Hibridação Fluorescente *in situ* (FISH) juntamente com os Mímicos de Ácidos Nucleicos (NAMs), tais como o *Locked Nucleic Acid* (LNA) e o 2'-O-Metill (2'OMe), tem vindo a ser desenvolvida para detetar e localizar rapidamente células microbianas gástricas. No entanto, o número de microrganismos que podem ser discriminados pela técnica tradicional de FISH é geralmente limitada a 3 alvos. Deste modo, outra tecnologia, a imagem espetral tem vindo a ser desenvolvida e permite a identificação de fluorocromos com espetros sobrepostos de forma a detetar vários microrganismos em simultâneo. A combinação do FISH com a imagem espetral e com sondas NAMs permitiu criar um procedimento mais simples para estudar a composição da microbiota diretamente no estômago.

Numa primeira fase, a sonda universal LNA/2'OMe foi acoplada a 8 fluorocromos fluorocromos diferentes (Alexa Fluor 405, Alexa Fluor 488, Alexa Fluor 514, ATTO 532, ATTO 550, Alexa Fluor 594, ATTO 633 e ATTO 655) elaborando-se o ranking das bactérias e dos fluorocromos, consequentemente atribuímos à bactéria que possuía maior intensidade de fluorescência o fluorocromo com menor intensidade e vice-versa Também se verificou que usando a imagem espetral no microscópio confocal LEICA TCS SP5, foi possível discriminar-se 7 fluorocromos simultaneamente numa única imagem quando se aplicou a técnica a 5 espécies bacterianas presentes na microbiota gástrica de ratinhos, à *H. pylori* e à *Citrobactrer freundii*. Para além disso, verificou-se também que utilizando esta metodologia, as bactérias são corretamente separadas já que a frequência após análise espetral é similar à frequência de células que foi efetivamente colocada na amostra.

Adicionalmente, foram também desenhadas sondas de LNA/2'OMe específicas para *C. freundii Muribaculum intentinale*, e *Faecalibaculum rodentium*, enquanto que sequências oligonucleotídicas presentes na literatura foram re-avaliadas para *H. pylori*, *Lactobacillus* sp., *Bacteroides* sp. e Clostridiales. Estas sondas beneficiam de elevada sensibilidade e especificidade e tempratuturas de melting de aproximadamente 77.5 ºC.

Esta metodologia demonstrou uma extraordinária capacidade para distinguir fluorocromos com espetros de emissão numa única imagem adquirida espectralmente após aplicação do algoritmo *linear unmixing*.

Palavras Chave: FISH, MIcrobiota Gástrica, LNA/2 OMe, NAMs Imagem Espetral

Declaration

I hereby declare, on my word of honor, that this work is original and that all non-original contributions were properly referenced with source identification.

Index

List of Figures

List of Tables

Glossary

ΔG º	Gibbs free energy change
2'OMe	2'-O-methyl
AF	Alexa Fluor
bp	Base pairs
CBA	Columbia Base Agar Base Medium
DGGE	Denaturing Gradient Gel Electrophoresis
DNA	Deoxyribonucleic acid
FISH	Fluorescence *in situ* Hybridization
I3S	*Instituto de investigação e Inovação em Saúde*
INIAV	*Instituto Nacional de Investigação Agrária e Veterinária*
INS-GAS	Transgenic insulin-gastrin
Jax	Jackson Laboratory
MRS	Man, Rogosa and Shape Agar Medium
NaCl	Sodium chloride
NAMs	Nucleic Acid Mimics
nPs	Non-target strains that did not react with the probe
PO	Phosphodiester oligonucleotides
PS	Phosphorothioate oligonucleotides
RNA	Ribonucleic acid
rRNA	Ribosomal ribonucleic acid
SPF	Specific Pathogen Free
spp.	Species
sS	Number of strains detected by the probe
Tac	Taconic Bioscience
TGGE	Temperature gradient gel electrophoresis
Tm	Melting temperature
tPs	Total of non- strains
ts	Theoretical specificity
TSB	Tryptic Soy Broth Medium
TSs	Total number of strains present in the databases

1 Work outline

1.1 Contextualization and Motivation

Evidence that the host microbiota specifically functions to promote health and prevent disease and that dysbiosis contributes to inflammation, susceptibility to pathogens, and diseases, including cancer, is undisputed (Noto et al., 2017).

Helicobacter pylori is the main cause of several gastroduodenal diseases. Despite its high prevalence, recent studies have demonstrated the presence of other bacterial species in gastric mucosa and gastric juice, which means that interactions between these species and *H. pylori* are possible (Alarcón et al., 2017; Testerman & Morris, 2014; Tsay & Hsu, 2018). Thus, it becomes essential to clarify this paradigm.

Thorough knowledge of the role microorganisms plays in the gastric microbiota, as well as its spatial location, is a subject on which researchers and physicians have bent over. Understanding how the microbial communities drive diseases or health could be the key factor to improve therapeutic strategies to combat or prevent gastric diseases; and for that, a technology that provides information about the spatial organization of the microbiota within stomach is paramount.

Despite the success of Fluorescence *in situ* Hybridization (FISH) in detecting and locating microorganisms, this technique suffers from limitations associated to the low multiplex capabilities, meaning that only two or three different types of microorganisms can be successfully distinguished in a single sample (Moter and Göbel 2000). Thus, to increase the number of distinguishable targets simultaneously, a recent technology, called spectral imaging-FISH is emerging (Valm et al., 2012b). In addition, the FISH technique suffers limitations associated to the use of DNA probes, which might be overcome taking advantage of the enhanced hybridization properties of Nucleic Acid Mimics (NAMs) (Cerqueira et al., 2008; Kubota et al., 2006).

Hence, combining spectral imaging-FISH with NAMs probes (LNA/2'OMe) will allow to create a more straightforward procedure to study the composition and spatial organization of the gastric microbiota, without disrupt the samples. This could provide information about the potential functions of each member involved in gastric microbiota.

1.2 Research objectives

The aims of this work are combining the FISH technique with spectral imaging and nucleic acid mimics to study the composition and spatial organization of the microbiota in the stomach, to better understand the role of microorganisms in the development of gastric diseases. For this, it is intended to rank the fluorochomes and bacteria, and match the bacteria displaying weaker fluorescence intensity with the brightest fluorochromes and vice-versa.

Furthermore, it intended to verify if the Leica TCS SP5 II Confocal at i3S allows to implement the technique, making a preliminary experiment with *E. coli*. Then, in order to optimize and implement this method, LNA/2'OMe probe coupled to 7 different fluorochromes is apply to 5 mouse gastric bacterial species, *H. pylori* and *Citrobacter freundii*.

Finally, it is intended design specific LNA/2'OMe probes to target the 16S ribosomal RNA sequences for all bacterial species involved in this study; for *Muribaculum intestinale*, *Faecalibaculum rodentium* and *C. freundii* were designed probes using PRIMROSE; for other bacteria (*H. pylori, Bacteorides* sp, *Lactobacillus* sp. and Clostridiales) the reported sequences will be re-evaluated.

1.3 Contributions of the Work

The work presented in this thesis was mainly done by me, except the fixation of the *Helicobacter pylori* (ATCC 700392 / 26695), *Clostridium innocuum* (DSM 26113) and *Clostridium sporogenes* (DSM 29420). These bacteria were fixed in *Instituto Nacional de Investigação Agrária e Veterinária* (INIAV) by Andreia Azevedo, as these are biosafety level two bacteria.

1.4 Organization of the Thesis

This work is divided in 5 chapters. The present chapter describes the main objectives, context and motivations for the development of this work and serves as a guideline to the overall work presented in the subsequent chapters.

In chapter 2 a brief literature review is provided. It focusses in gastric microbiota and mouse models, and molecular tools for its study. Furthermore, this chapter includes a description of the Fluorescence *in situ* hybridization technique, which includes a description

of its technical aspects and possible drawbacks. Taking into account the advantages of NAMs (e.g. LNA and 2'OMe) and the high potential of spectral imaging to improve the FISH, a review of LNA and 2'OMe molecules, and spectral imaging was also included.

Chapter 3 consists in the Materials and Methods section used during this work, providing details about culture maintenance, hybridization procedures in suspension, spectral image acquisition and evaluation of the relative fluorescence intensities using the Fiji software. It is also described how the *in silico* LNA/2'OMe probes were designed and evaluated in terms of its theoretical performance.

Chapter 4 comprises the results obtained during the work and a discussion regarding aspects such as the optimization of the hybridization solution, ranking of fluorochromes and bacteria, spectral imaging to discriminate 8 fluorochromes with highly overlapping emission spectra, LNA/2'OMe probes design and its theoretical evaluation.

Finally, chapter 5 present concluding remarks. In chapter 6 an analysis of the goals achieved, limitations and future work for further research is described.

2 Literature Review

2.1 Gastric Microbiota

The human gastric microbiota harbors a diverse and complex microbial community which plays a fundamental role in human health (Ursell et al., 2012). The microbiota performances a major role in healthiness and diseases, and it is associated to energy reap and storage, as well as, to a variety of metabolic functions such as fermenting and absorbing carbohydrates (Clemente et al., 2012).

Gastric adenocarcinoma is the third leading cause of cancer death worldwide, accounting for more than 720000 deaths annually (Noto et al., 2017). Among the different risk factors that increase the risk of developing this disease, *H. pylori* plays a crucial role in the initial steps of carcinogenesis (Ishaq and Nunn 2015; Ferreira et al. 2018; Atherton and Blaser 2009).

H. pylori is a Gram-negative bacterium, spiral microaerophilic that colonizes the gastric mucosa of at least 50% of the worldwide population (Velin and Michetti 2006), and it can frequently be acquired in childhood and, if not treated can persist throughout lifetime (Atherton and Blaser 2009). The infection with *H. pylori* can have different consequences, according with the genetics of the bacterial strain and also the type of inflammatory response of the host (Atherton & Blaser, 2009; Figueiredo, 2002; Petra et al., 2017).

The stomach was considered to be a sterile organ until the discovery of *H. pylori*. However, recent studies have showed that other microorganisms beyond *H. pylori* can colonize the gastric mucosa despite its acidic environment (pH is about 1.4) (Alarcón et al., 2017; Wu et al., 2014). In fact, the high acidity of stomach prevents the survival and proliferation of bacteria (Cotter and Hill 2003). However, the gastric mucus creates a pH gradient thus providing safeguard of bacteria from acid attack (Wang et al. 2014).

H. pylori infection usually does not alter the acid barrier of the gastric mucosa, unless an unregulated inflammatory response in the corpus leads to atrophy and hypochloridria (Aviles-Jimenez et al., 2015).

Long term *H. pylori* infection leads to gastric atrophy, and consequently, to an increase of the gastric pH, which stimulates the colonization of the stomach by transient bacteria (Nardone and Compare 2015a). In addition, *H. pylori* produce ammonia and bicarbonate from urea that have been implicated in the pathogenesis of *H. pylori* infection because may serve as substrate for the other bacteria (Kusters et al., 2006; Nardone & Compare, 2015a).

The microbial communities of the stomach have not been studied in detail; it was demonstrated that other microorganisms present in the stomach may play a relevant role in the behavior of *H. pylori* and vice-verse, thus influencing the disease / health (Kienesberger et al. 2016). The gastric microbiota consists of bacteria from seven to eleven phyla, predominantly Proteobacteria, Firmicutes, Bacteroidetes, Actinobacteria and Fusobacteria, however these composition vary remarkably between individuals and studies (Wang et al. 2014; Thursby and Juge 2017).

However, the effect of *H. pylori* on the microbiota of the human stomach has been examined in a limited number of studies. It was reported that *H. pylori* had no effect on the composition of the adult human gastric microbiota (Bik et al. 2006), whereas it was showed that *H. pylori*-infected adults tended to have a higher abundance of non-*Helicobacter* bacteria from Spirochetes, Acidobacteria and Proteobacteria with a relative decrease in members of the Actinobacteria, Bacteroidetes and Firmicutes compared with uninfected adult subjects (Maldonado-Contreras et al. 2011).

The effect of *H. pylori* on the composition of the gastric microbiota is incompletely understood (Brawner et al., 2014). It is essential to study the relationships between microorganisms and between them and the host, their role in the community and their influence on the development of infection (Figure 2.1).

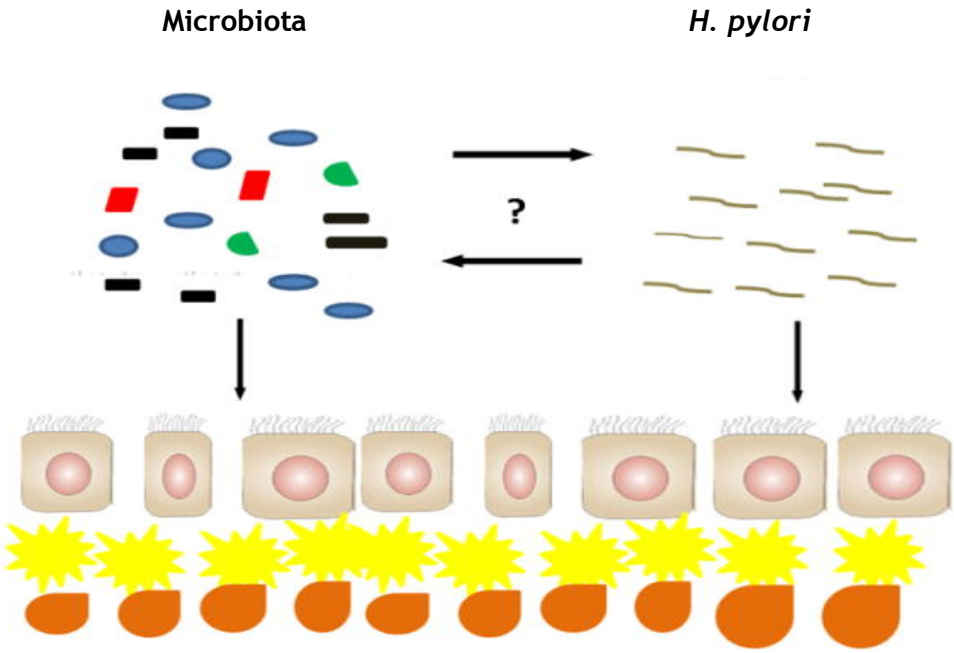

Figure 2.1. Interaction between *H. pylori* and microbiota. The study of microbial interactions between *H. pylori* and non-*H. pylori* species might provide important information about their role on disease and health. Adapted from Brawner et al., (2014).

By exploring the structures and dynamics of gastric microbiota, the relationships between *H. pylori* and non-*H. pylori* species will allow to analyze the spatial organization of

gastric microbiota, identifying the preferred locations of the microorganisms within stomach and providing crucial information about the potential function of each member involved in microbiota. This could be the key factor to improve therapeutic strategies to combat or prevent gastric diseases (Engstrand and Lindberg 2013).

In gastric microbiota research, mouse models have been increasingly used to study the role and functioning of the gastric microbiota, the interaction of microbes with their host and its connection with diseases (Hörmannsperger et al., 2015; Hugenholtz & de Vos, 2018).

2.1.1 Studying the gastric microbiota using mouse models

Mouse and human are quite similar in physiology and anatomical structures, and this is one of the reasons why mouse models have been widely used in studies (Andersen and Winter 2019). Specifically, the gastrointestinal tracts in both species are constituted of organs that are anatomically similar. However, the anatomy of the human and mouse gastrointestinal tract also have obvious differences, which might be shaped by their diverging diets, body sizes, feeding patterns and metabolic requirements (Nguyen et al, 2015; Treuting & Dintzis, 2012).

The mouse stomach is divided in two cavities: glandular stomach and non-glandular stomach, (Figure 2.2.A). A glandular stomach is responsible for secreting gastric acid, whereas the non—glandular stomach functions as temporary site of food storage and digestion. The human stomach is lined with a glandular mucosa (Figure 2.2.B) that secretes gastric acid (Nguyen et al. 2015; Hugenholtz and de Vos 2018).

Figure 2.2. Anatomy of the mouse and human stomach. In the left side the stomach of the mouse and the right side the human stomach. Adapted from Nguyen et al., (2015).

Although results from experiments in mouse models have yielded important breakthroughs in understanding the dynamic and complex relationships between the gastric microbiota and its host, converting such results from murine models to humans remains nontrivial due to the existence of some fundamental differences between the two systems that need to be taken into account (Hörmannsperger, Schaubeck, and Haller 2015).

The ability to establish causality is greatly enhanced by carefully controlled and manipulatable animal models systems (Noto, Peek, and Jr. 2017). The progressive knowledge of mouse genetics and the availability of numerous genetically modified mouse models, the large similarities in anatomy, genetics and physiology greatly facilitate functional studies have allowed several inferences about human biology to be drawn from mouse experimentation (Ruiz et al., 2017).

Moreover, mouse is the model of choice not just because they are interestingly similar to humans at the genomic level, but also because the pathophysiology of disease in mice is similar to that of humans (Takao and Miyakawa 2015). Furthermore, mouse models present low maintenance cost as compared with other mammalian experimental models, high reproductive rates, short life cycle (about two years in laboratory) and they are relatively easy to handle and transport (Perlman 2016).

Experimental manipulations of mouse models in gastric microbiota research follow functional and mechanistic research on host-microbe interactions, thus helping to assess causality in disease-associated alterations in gastric microbiota composition. Manipulations that are essential to gastric microbiota research include host genetic background manipulation (gene knockouts), gastric microbiota composition manipulation (controlled inoculation in germ-free or gnotobiotic mice, i.e., germ-free mice administered with external microbes) and ecosystem interventions including dietary interventions and antibiotic treatment (Nguyen et al. 2015).

In healthy mices, *Veillonella* sp., *Lactobacillus* sp. and *Clostridium* sp. are the most frequently isolated bacteria from the gastric mucosa (Wang et al. 2014). C57BL/6 mice have been widely used in biological and biomedical research due to the in-depth knowledge of their genetic profile and their use in an array of transgenic mouse strains (Andersen and Winter 2017). The gastric microbiota of C57BL/6 mice is dominated by the same predominant phyla that have been reported in humans: Firmicutes, Bacteroidetes, Proteobacteria and Actinobacteria (Noto, Peek, and Jr. 2017). At the genera level, the healthy human stomach is dominated by *Haemophilus, Prevotella, Rothia, Streptococcus and Veilonella* (Noto, Peek, and Jr. 2017; Nardone and Compare 2015b). In contrast, in the BALB/c mice the most frequently occurring genera in the stomach were *Lactobacillus* sp., *Streptococcus* sp. and *Bacteroides* sp. (Brown and Balish 1978). On the other hand, a study using INS-GAS mice demonstrated the presence of *Clostridium* sp., *Lactobacillus* sp. and *Bacteroides* sp. (Whary et al. 2014).

A distinct microbiota was observed in C57BL/7 mice from Jackson laboratory (Jax) and Taconic Bioscience (Tac). Most notably, segmented filamentous bacteria, a group of spore-forming Gram-positive bacteria, are present in Tac mice but absent from Jax mice (Ge

et al. 2018). Consequently, these mice developed different pathological an immunological response to *H. pylori* infection.

It has been documented that effects of *H. pylori* infection on the gastrointestinal bacterial community structures are variable in different mouse strains (Ge et al. 2018).

In specific pathogen free (SPF) BALB/c mice, the colonization by *H. pylori* results in the reduced abundance of *Lactobacillus* sp. In transgenic insulin-gastrin (INS-GAS) mice, *H. pylori* infection elevated abundance of Firmicutes and a reduction in Bacteroidetes. In contrast, *H. pylori* infection had no effect on the gastric microbiota in conventional C57BL/6 mice (Cao and Yu 2015; Lofgren et al. 2011; Ge et al. 2018).

The ability of *H. pylori* to alter the gastric microbiota of mice is likely determined by several factors, including the genetic background of the mouse, the strain of *H. pylori*, and the length of infection (Brawner, Morrow, and Smith 2014; Lofgren et al. 2011). Despite the relatively low *H. pylori* abundance in mice compared to humans, physiology and immunity were substantially affected (Kienesberger et al. 2016).

However, animal testing is not an alternative to human trials, it only complements it. These combinations of features provide researchers with a uniquely powerful tool for understanding the mechanisms of human disease and testing of novel drug therapies (Takao and Miyakawa 2015). To determine cause versus effect, studies may also need to integrate humanized mouse models has been brought more insights into the pathological mechanisms to understand effects of the human gastric microbiome on disease (Noto, Peek, and Jr. 2017).

2.2 Molecular tools to study gastric microbiota

Understanding the composition and functional capacity of the gastric microbiota represents a major challenge. However, research in this area is ever expanding and currently a number of different approaches are being used and developed to determine gastric microbial composition, genetic content and microbial function (Guinane and Cotter 2013).

Different methodologies have been used to identify microorganisms in the stomach. Firstly, characterization of the human gastric microbiota was traditionally relied on cultivation of gastric juice or mucosal biopsies, before the introduction of molecular techniques (Stark et al. 1996; Savage 1977). Investigation of non-*H. pylori* treatment to study the ecological effect on the gastric microbiota (Adamsson et al., 1999) and studies of co-existents rates of *Lactobacillus spp*. and *H. pylori* in the stomach (Roos et al., 2005) are examples where culture-based techniques have been used. The gastric samples were

inoculated on selective and non-selective agar media and incubated both anaerobically and aerobically. In addition, mass spectrometry for the identification of pathogenic bacteria acquired after culture are usually used as a complement to standard identification procedures (Engstrand and Lindberg 2013).

However, these techniques underestimate the biodiversity of bacteria, as a great part of them cannot be cultured (Vartoukian et al., 2010).

The role of the gastric microbiota in human health and disease is becoming clearer due to the recent introduction of high throughput sequencing technologies as well as parallel recent developments in nongenomic techniques that demonstrate the existence of a complex microbiota in human stomach dominated by *Prevotella*, *Streptococcus*, *Veillonella*, *Rothia* and *Haemophilus*. In *H. pylori* infected stomach was observed a shift in abundance of Firmicutes phyla, *Prevotella* and *Streptococcus* genera (Li et al., 2009; Maldonado-Contreras et al., 2011).

As a consequence, several culture-independent molecular methods based on 16S rRNA genes have been developed, such as denaturing or temperature gradient gel electrophoresis (DGGE and TGGE), dot blot hybridization with rRNA-target probes, cloning and sequencing of rDNA and DNA Microarrays for the identification and classification of gastric bacteria (Nardone & Compare, 2015a; Yang et al., 2013).

A pioneer study using TGGE of PCR-amplified 16S rDNA fragments showed that *Enterococcus, Pseudomonas, Staphylococcus, Streptococcus* and *Stomatococcus* are the most abundant genera present in human stomach (Kraft et al., 2000). Although many of these bacteria also inhabit the oral cavity and respiratory tract, the presence of *Pseudomonas* sp. other than *Pseudomonas aeruginosa* has led to the assertion that the gastric environment contains a native microbiota (Bik et al. 2006). Furthermore, gastric biopsy samples were analyzed by using a small subunit 16S rDNA clone library approach, and identified five different bacterial phyla: Proteobacteria, Firmicutes, Actinobacteria, Bacteroidetes and Fusobacteria (Petra, Rus, and Dumitrașcu 2017).

On the other hand, Delgado et al., (2013), combining culture-independent and classical culturing techniques, have reported the most abundant genera belonged to *Streptococcus, Propionibacterium and Lactobacillus* (Delgado et al. 2013).

However, the use of these techniques to study the composition of microbiota in gastric biopsies or in model animals, disrupt the spatial structure of the samples, meaning that important information about structure and ecology of the gastric microbiota might be lost. In addition, the time needed to process a sample is quite long, making these methods less suitable as a diagnostic routine (Fontenete et al. 2013).

Thus, to identify which species are present and where, what they are doing, and how densities of the species change over time, there is necessary pressing for a technical advancement to provide a structural analysis of the microbiota spatial organization within the stomach without disturb the microbial communities. As such, Fluorescence *in situ* Hybridization (FISH) has been applied for the detection and location of *H. pylori* directly in stomach.

2.3 Fluorescence *In Situ* Hybridization

FISH is a powerful molecular technique that allows the simultaneous visualization, identification, quantification and localization of microorganisms (Moter and Göbel 2000).

A timeline of the evolution of the FISH procedure is shown in Figure 2.3.

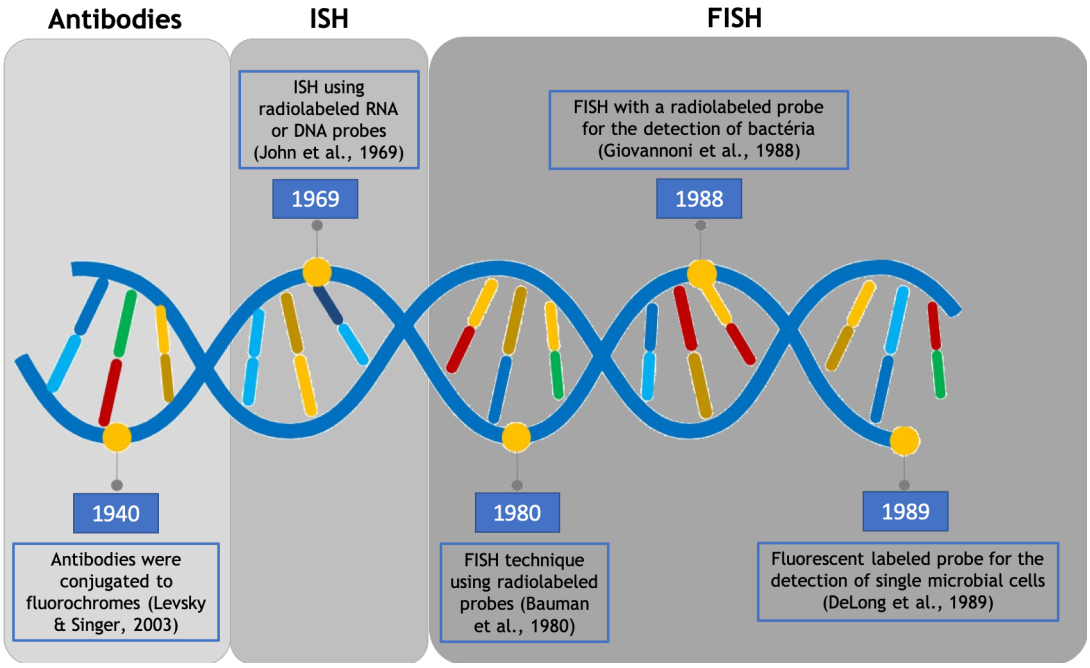

Figure 2.3. Timeline of the evolution of the FISH procedure, starting with the antibodies conjugated to fluorochromes until the fluorescence *in situ* hybridization (FISH).

The first ability to detect specific molecular identities was demonstrated by antigen-antibody interactions. In the 1940s, antibodies were conjugated to fluorochromes without losing their epitope-binding specificity (Levsky and Singer 2003). Later, in 1977, the first antibody-dependent fluorescent detection of nucleic acid hybrids was accomplished (Rudkin and Stollar 1977). This technology was soon replaced by the development of fluorescent acid probes (Levsky and Singer 2003).

The earliest *In Situ* Hybridization (ISH) implemented in the late 1960s by John et al., (1969) and Pardue & Gall, (1969) demonstrated the hybridization of radioactive labelled RNA and DNA probes to the target DNA sequences in mammalian cells.

In 1980 was described the first application of FISH, with a RNA probe for a specific DNA sequence labelled with a fluorochrome directly to the 3' end of probe (Bauman et al., 1980). Subsequent, Giovannoni et al., (1988) described the detection of bacteria using radiolabeled probe capable of detecting single cells. In 1989, it was used the first fluorescently-labelled oligodeoxynucleotides complementary to 16S rRNA for the detection of single microbial cells (DeLong et al., 1989). The fluorescent probes allowed significant advanced in terms of speed and safety. In addition, the fluorescent probes can be labelled with dyes of different emission wavelengths (Moter and Göbel 2000).

Then, FISH has been used for the detection of microorganisms in complex environments such as oral cavity (Mendes et al. 2016), intestinal and gastric biopsy (Cerqueira et al., 2013; Nordentoft et al., 1997; Tropini et al., 2017), respiratory tract infections (Hogardt et al. 2000), blood samples (Jansen et al., 2000; Kempf at al., 2000), urinary tract infections (Wu et al., 2010) and in diverse environmental samples such as sea sediments (Llobet-Brossa et al., 1998).

Typically, the probes used in FISH methods are oligonucleotide sequences between 15 and 30 base pairs (bp) in length, with a single fluorescent molecule covalently attached to the 5' or 3' terminus (Moter and Göbel 2000; Yaroslavsky and Smolina 2013).

The FISH technique for Bacteria or Archaea is based on the hybridization of a labelled-probe, usually DNA, with a target molecule, usually the 16S ribosomal RNA sequence; the probes for Eukaryotes domain, most common used are the 18S rRNA sequence, but 26S is also used for some microorganisms (Fukuda et al., 2016). The rRNA is chosen as a common target molecule due to its relatively stable, its domain structure with conserved and variable regions, and its high abundance in the cell and, consequently, high fluorescence intensities are obtained as a result (Amann et al., 2001; Amann & Fuchs, 2008; Woese, 1987).

Labelling of the probes can be performed in two different ways: "direct labelling" and "indirect labelling" (Morrison et al., 2002; Moter & Göbel, 2000). In "direct labelling", the probe is labelled directly with the fluorochromes by a chemical conjugation between the fluorochrome and the nucleic acid, while in "indirect labelling", the chemical conjugation of the nucleic acid is to a non-fluorescent molecule that can bind fluorescent material after hybridization (Moter and Göbel 2000; Fan 2002). "Direct labeling" is the fastest, cheapest and easiest way of labeling because does not entail any further steps after hybridization (Moter & Göbel, 2000).

Basically, the procedure of FISH consists on the detection of nucleic acids sequences through fluorescently labelled nucleic acid probe, which hybridizes specifically to the complementary target sequences within intact cells (Moter and Göbel 2000; Yaroslavsky and Smolina 2013).

The procedure includes the following steps: fixation, permeabilization, hybridization, washing and visualization (Moter and Göbel 2000; Cerqueira et al. 2008; Fontenete et al. 2015). A short outline of procedure is illustrated in Figure 2.4.

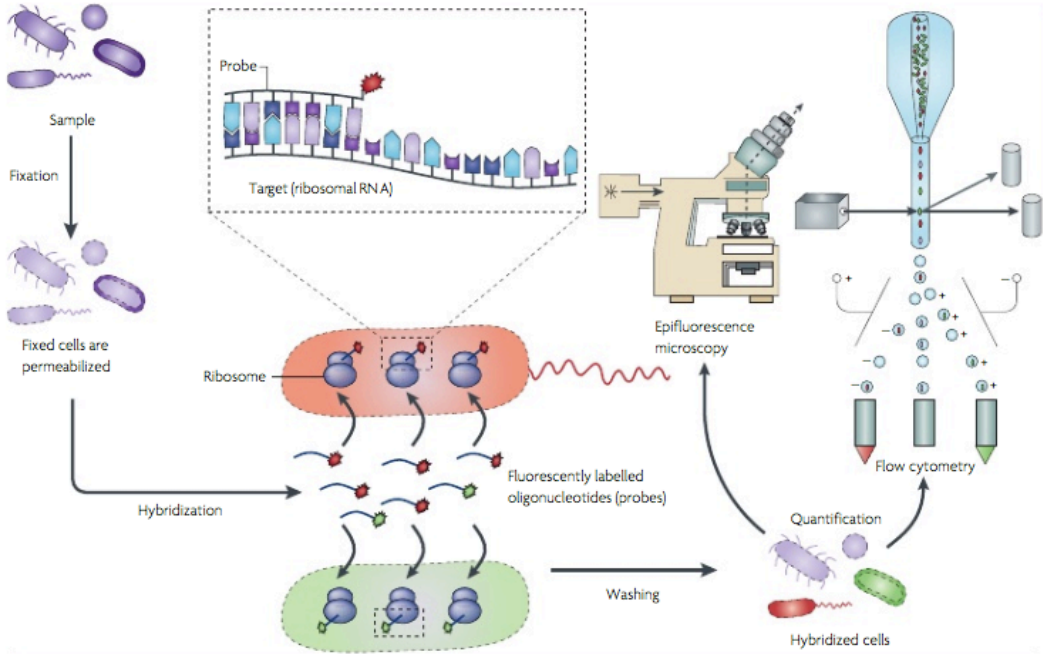

Figure 2.4. Schematic of basic steps of Fluorescence *in situ* Hybridization.The procedure includes the following steps: fixation and permeabilization of the samples that might includes specific pretreatment steps to render the cell wall permeable to the probe entry; the sample is then incubated with a fluorescently labeled probe that is complementary to species-specific regions of rRNA molecules; hybridized cells are then washed to remove excess probe or unbound probes or loosely bound probes; finally, analysis is perfomed by epifluorescence microscopyor flow cytometry. Reprinted from R Amann et al., (2001).

Fixation is crucial for satisfactory results in FISH; the samples containing microorganisms are fixed to protect RNA from degradation of endogenous RNAs, and the permeabilization step allows the probe to penetrate the cell. The fixation may use precipitating agents such as ethanol and methanol, or cross-linking agents like aldehydes. In the hybridization step, the probe penetrates the cell and binds to the target region of the rRNA. During the hybridization step, temperature, pH, ionic strength and denaturant concentrations should be well-defined to guarantee that the probe accesses and hybridizes with the target sequence (Cerqueira et al., 2008; Moter & Göbel, 2000). Then, the washing step is needed to remove unbound probe or probe which has loosely bound to the target. Finally, a specific filter or laser is used, depending on the fluorochrome used, to visualize microorganisms using epifluorescence microscopy or flow cytometry (Frickmann et al., 2017; Moter & Göbel, 2000; Rocha et al., 2018); the fluorescence signal emitted by the fluorochrome-probe-target complex allows a visual detection of the microorganisms.

However, the application of FISH assumes some limitation based on the false negative and false positive results (Moter and Göbel 2000).

The main cause of false negative results is the probes **inability to penetrate the cell wall**, **photobleaching, use of bacterial probes, low rRNA content** and **higher order structure of target or probe**.

- **Inability to penetrate the cell wall**

Low signal intensity may be the consequence of insufficient probe penetration and depends the structure of the bacterial cell wall. Sometimes, in the case of Gram-positive bacteria, enzymatic treatments are performed with lysozyme or other proteolytic enzymes, in order to promote the disintegration of the peptidoglycan, allowing the probe to penetrate the cell and, consequently, a more fluorescent signal (Silverman and Kool 2007; Moter and Göbel 2000).

- **Photobleaching**

Fluorochromes-labeled probes also are prone to photobleaching during preparation and hybridization, so care must be taken to avoid prolonged exposure to strong light; with exposure times of several seconds or even minutes, this may have a critical effect (Moter & Göbel, 2000).

- **Use of bacterial probes**

Eubacterial probe EUB338 is the most commonly used to gives satisfactory results in FISH method and to control false negative results. However, this probe does not detect some bacterial phyla including Planctomycetales and Verrucomicrobia. Consequently it might be necessary to use a set of bacterial probes to get a more comprehensive view when analyzing complex microbial communities (Moter & Göbel, 2000).

- **Low rRNA content and higher order structure of target or probe**

Normally, rRNA content is higher within cell but it varies considerably between species and also within cells of one strain according to their metabolic and physiologic state. (Bottari et al., 2006; Stender et al., 2002). Loop and hairpin formation as well as rRNA-protein interactions obstructs hybridization and lead to differential signal intensity of oligonucleotide probes (Moter and Göbel 2000).

Furthermore, false positive results happen due to **autofluorescence** and **lack of specificity**.

- **Lack of specificity**

Precision of FISH depends on the design of the probe. Probe design is usually done by recurring to sequencing databases, if designing is performed using a database that is not the

most recent update, it could lead to a mistake in the sequence selected for the probe, and consequently a non-specific sequence for the selected microorganisms.(Bhatia et al,. 1997).

- **Autofluorescence**

In FISH, one of the most problems is autofluorescence of microorganisms and controls need to be done in order to assess if the microorganism has or not autofluorescence (Margo and Bombardier 1985). Many times, growth media, fixation of bacteria and mounting media seem to have dramatic influence on the signal intensities.

However, the FISH techniques suffer from limitations associated to the use of DNA probes, such as low affinity of the probe for its targets, low robustness and degradation of the probe by endonucleases of living cells (Kubota et al., 2006). Thus, this technique might be overcome taking advantage of the enhanced hybridization properties of Nucleic Acid Mimics (NAMs) (section 2.3.1) (Cerqueira et al., 2008; Nielsen et al., 1991; Petersen & Wengel, 2003).

In addition, many fluorochromes have highly overlapping excitation and emission spectral (Ferrer and Mira 2016). As a result, limited number of reporter fluorescent molecules can be discriminated (usually limited to two or three colors) (Pautke et al., 2007; Valm, Mark Welch, & Borisy, 2012; Valm, Oldenbourg, & Borisy, 2016). In order to address this issue, another technology, named Spectral Imaging is emerging to solve this issue (section 2.3.2) (Pautke et al., 2007; Valm et al., 2012; Valm et al., 2016).

2.3.1 Nucleic Acid Mimics: Locked Nucleic Acids (LNA) and 2'O-methyl-RNA (2'OMe)

The NAMs, including Peptide Nucleic Acid (PNA), Locked Nucleic Acid (LNA), and 2'-O-methyl-RNA (2'OMe), takes benefits including resistance to the attack of enzymes due to their synthetic nature, higher affinity for RNA sequences with a lower number of base pairs, which leads not only to more successful hybridizations but also to easier discrimination of single-base mismatch (Kubota et al. 2006; Fontenete et al. 2015).

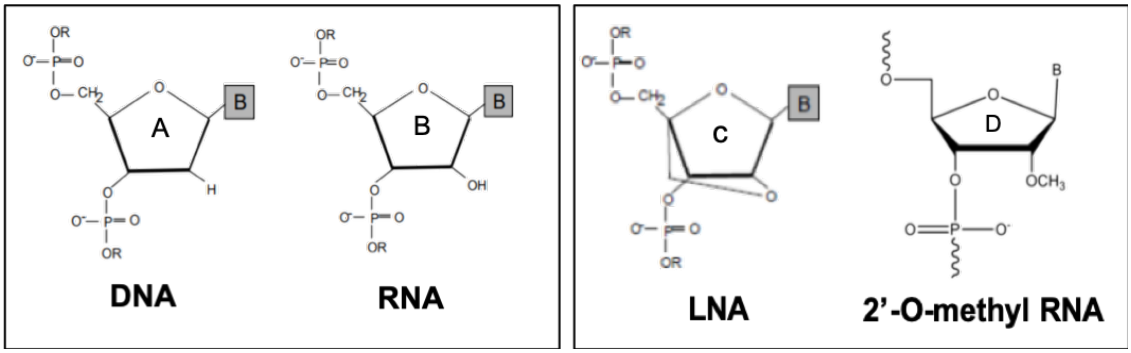

Figure 2.5. Chemical Structures of DNA, RNA LNA and 2'OMe mimics. A- DNA; B- RNA; C-Locked Nucleic Acid (LNA). D- 2'OMethyl. Adapted from Younger & Corey, (2009).

LNA (Figure 2.5.C) represent a class of RNA analogs that have an especially high affinity towards complementary DNA and RNA (Silahtaroglu et al., 2004). LNA is a synthetic RNA derivate nucleotide analog in which the ribose is connected to a methylene bridge between 2'-oxigen and 4'-carbon atoms, that is, formed with 2'-O,4'-C-methylene-ß-D-ribofuranosyl nucleotides. The association encompasses the sugar, which is accountable for the new conformation that is better for the configuration of hybrids with complementary DNA or RNA sequences (Cerqueira et al. 2008).

Replacement of DNA probes with LNA has exhibited to considerably increase their thermal duplex stability as well as to improve the discrimination between flawlessly matched and mismatched target nucleic acids (Silahtaroglu et al. 2004; Wahlestedt et al. 2000). In fact, it has been shown by thermal studies that DNA duplexes containing LNA residues have the ability to increase the melting temperature (Tm) between 2 ºC and 10 ºC per single LNA nucleotide incorporation (Cerqueira et al. 2008).

LNA monomers can be intercalated with DNA or other NAMs, which leads to greater hybridization efficiency in the FISH technique (Fontenete et al. 2016; Kubota et al. 2006).

2'OMe RNA (Figure 2.5.D) constitute another NAM that is being used as a diagnostic probe in animal cells. The 2'OMe group induces relatively high affinity towards an RNA target likely due to the C3'-endoconformation adopted by 2'OMe ribose sugars (Fontenete et al. 2013).

2'OMe is a naturally appearing modification found in RNA that increases affinity for RNA targets due to the preference of 2'OMe-modified ribose sugars to adopt a C3'-endoconformation (Majlessi et al., 1998).

2'-OMe-RNA probes have showed high affinity, improved hybridization, increased specificity and capacity to bind RNA target sequences. In fact, these probes form more stable complexes with complementary RNA sequences than natural DNA and RNA probes. Due their

synthetic nature, 2'-OMe-RNA possess increased resistance to enzymes such as nucleases (Cerqueira et al. 2008).

Recent studies indicate that the substitution of DNA monomers by 2′-OMe-RNA monomers leads to superior hybridization efficiency in FISH (Fontenete et al., 2015).

In fact, the introduce of LNA monomers into 2'OMe probes enhance the target affinity even further due to an additive effect on the melting temperature (Fontenete et al. 2016). In terms of FISH experiments, the LNA/2'OMe design allows increase of fluorescence intensities relatively to LNA designs (Fontenete et al. 2016). In addition, using LNA molecules to control of annealing temperature becomes easier by doing mixed synthesis (intercalation of LNA nucleotides with DNA or other mimics); this allows for a control of the thermodynamic parameters, simplifying detection of multiple targets simultaneously (Azevedo et al., 2018).

However, other types of modifications may also be incorporated to improve the target's applicability. The use of phosphorothioate oligonucleotides (PS) exhibited some particularly interesting results in the case of human clinical samples. The PS monomers include substitute of one of the two non-bridging oxygen atoms by a sulfur atom at each internucleotide linkage. These types of oligonucleotides have an increased resistance to exonucleases and endonucleases when compared to phosphodiester oligonucleotides (PO), and are particularly appropriate for *in vivo* applications due to their longer elimination half-life (Fontenete et al. 2013).

In conclusion, LNA/2'OMe probes are very effective in multiplex approaches because with these synthetic molecules, it was possible to control the thermodynamic parameters of molecules, designing probes that work at specific conditions (e.g. at human body temperature (Fontenete et al. 2013)) or at same conditions (e.g. simultaneously detection (Azevedo, 2015; Azevedo et al., 2018)).

2.3.2 Spectral Imaging

The discovery and evolution of genetically encoded fluorescent reporters has revolutionized live-cell imaging. The number of spectrally variant fluorescent proteins and vital fluorochromes is large and ever increasing. Gradually, experiments are incorporating numerous fluorescent probes within single cells or tissues to define the distribution of more than one labeled structure or molecular species (Valm et al., 2016a). Such multi-color or multi-spectral imaging experiments require adequate separation of the fluorescent emissions, and this is especially problematic when the spectra are substantially overlapping (Valm, Oldenbourg, and Borisy 2016a).

However, the capability to distinguish more than a few different fluorescent reporters in a single sample is severely hampered by considerable overlap of their excitation and emission spectra (Cohen et al., 2018).

As each fluorochrome has its characteristic spectral profile, this signature can serve as a reference in multicolor approaches, Figure 2.6, (Kraus et al., 2007).

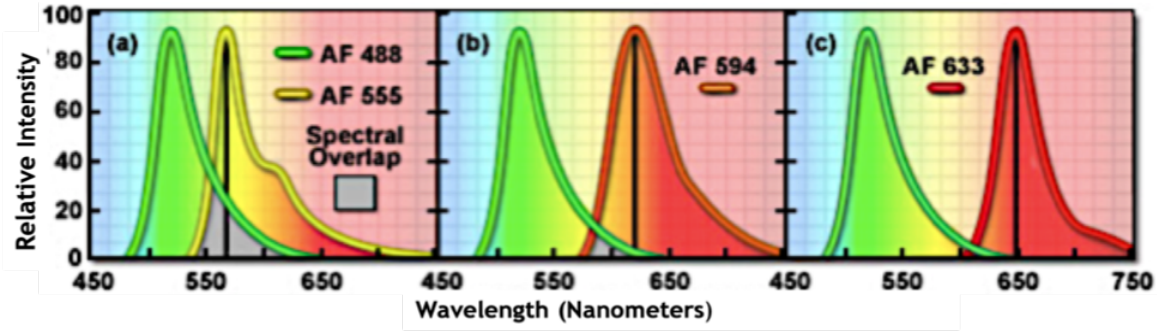

Figure 2.6. Spectral overlap in paired Alexa Fluor probes. The spectral overlap of fluorochromes decreases with increased wavelength. Reprinted from Murphy et al., (2017).

The emission spectra for the Alexa Fluor 488 and Alexa Fluor 555 fluorochromes (Figure 2.6.(a)) show a clear separation of the peak wavelengths, which are also easily distinguished by the human eye in green and yellow fluorescent light, respectively. However, the moderate level of spectral overlap (gray shaded area) illustrates that there is a considerable amount of emission from Alexa Fluor 488 at the peak emission wavelength of Alexa Fluor 555 (denoted by a black line running from the emission peak to the abscissa). This high level of signal bleed-though renders separation of the probes difficult in situations where the fluorescence emission intensity of Alexa Fluor 488 is significantly greater that Alexa Fluor 555. However, the spectral overlap between Alexa Fluor probes decrease as the bandwidth between emission maxima increases, as showed in Figure 2.6.(b) and (c). In this case, Alexa Fluor 488 and Alexa Fluor 594 easily distinguishable to the human eye and the low degree of spectral overlap should yield good results with minimal bleed-through in multiplex experiments. Possibly, the best spectral separation in visible-light emitting Alexa Fluor dyes is the comparison between Alexa Fluor 488 and Alexa Fluor 633 (Figure 2.6.(c)).

Thus, fluorescence spectral imaging is recent technology that allows many different spectrally variant fluorescent markers to be distinguished in a single sample (Cohen, Valm, and Lippincott-Schwartz 2018).

With this technique, no longer an optical separation of signals into channels with non-overlapping bands is attempted but a recording of the complete emission signals from multiple fluorochromes is carried out. The most essential part of spectral imaging microscopy systems is a spectral dispersion element that separates the incident light into its spectral components, Figure 2.7 (Kraus, Ziegler, and Wolff 2007).

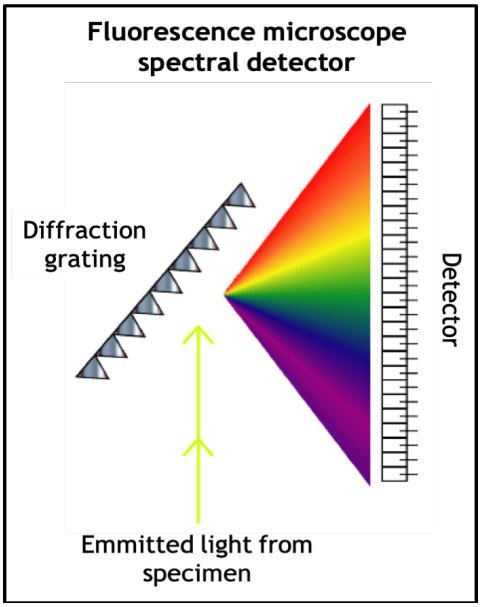

Figure 2.7. Schematic of an example spectral detector. Emitted light from the specimen is directed to a reflective diffraction grating. The grating sits in front of a linear array of photomultiplier tube (PMT) elements. Each element records emitted light over a specific visible wavelength bandwidth. Reprinted from: Valm et al., (2012b).

The most widely used approach for spectral deconvolution of images, called linear unmixing, involves a matrix inverse operation to find the best fit to known fluorochrome spectra to that of the recorded spectrum at every pixel in a digital image (Cohen, Valm, and Lippincott-Schwartz 2018).

Hence, advancements in fluorescence spectral image acquisition and the application of linear unmixing to spectrally documented image data extends the possibilities to discriminate different fluorochrome with overlapping spectra and consequentially the possibilities of multicolor imaging (Zimmermann et al. 2003).

In spectral unmixing, the emission spectrum of each fluorochrome is described in the form of a plot of its fluorescence emission intensity as a function of wavelength (James, 2006). Spectral imaging combines two methodologies: imaging and spectroscopy; imaging provides the intensity at every pixel of the image, and spectrometer provides a singles spectrum (Zimmermann, Rietdorf, and Pepperkok 2003). Thus, a spectral imaging provides a spectrum at each pixel that utilizes hardware to separate the emitted light into its spectral components (Garini et al., 2006; Tsurui et al., 2000).

On the other hand, linear unmixing is a computational process related to deconvolution that uses the spectra of each fluorochrome as though it were a point-spread function at a fixed location to “unmix” the component signals (Ikoma et al.,2014; Lansford et al., 2001). Thus, linear unmixing is applied to the spectral images to generate multichannel images in which each channel consists of measured intensities assigned to one of the distinct fluorochromes used (Hiraoka et al., 2002; Rieken et al., 2011).

This method is largely limited by factors such as detector noise or image background, however the appropriate selection of the number and bandwidth of the detection channels with respect to the overlap of the fluorochromes to be distinguished also plays an important role (Dickinson et al., 2014).

Spectral Imaging combined with FISH was already applied to the simultaneous identification of diverse microorganisms in a single image such as microbial population in complex biofilms (Almstrand et al., 2013), in colon biofilms (Dejea et al. 2014), in specific bacteria from seawater (Hasegawa et al. 2010) and in oral microbiome (Valm et al., 2012b; Valm et al., 2016b; Vogt et al., 2006). Thus, this methodology seems to be tailored for the study the gastric microbiota

3 Materials and Methods

3.1 Selection of the fluorochromes and mouse gastric bacterial species

Firstly, were selected the fluorochromes to be attached to the FISH probes, according the laser lines available on the Laser Scanning Confocal Microscope Leica TCS SP5 II and their spectral properties (Leica Microsystems, Germany). Hence, the fluorochromes selected were: Alexa Fluor 405, Alexa Fluor 488, Alexa Fluor 514, ATTO 532, ATTO 550, Alexa Fluor 594, ATTO 633 and ATTO 655.

The selection of the bacterial species was made according the sequencing results of 4 gastric samples of 4 C57BL/6 mice (2 males and 2 females of 9 weeks of age), (please, see Appendix 1). Thus, the bacterial species used in this study were: *Lactobacillus murinus* DSM 28683, *Lactobacillus paracasei* DSM 28675, *Muribaculum intestinale* DSM 28989, *Faecalibaculum rodentium* DSM 103405, *Anaerotruncus colihominis* DSM 28734, *Acutalibacter muris* DSM 26090, *Clostridioides mangenotii* DSM 29133, *Clostridium beijerinckii* DSM 791, *Bacteroides caecimuris* DSM 26085 and *Bacteroides dorei* DSM 17855. Additionally, *Helicobacter pylori* (ATCC 700392 / 26695) and *C. freundii* (ATCC 8090) were used in this experiment because, in future, *in vivo* studies will be attempted, to study how gastric microbiota change over time in the presence of these bacteria.

3.2 Bacterial strains and culture conditions

Each bacterial strain used in this work was grown according the culture conditions described in the Table 3.1.

Table 3.1. Growth conditions and incubation time for each bacteria

Bacteria	Culture Growth conditions	Incubation Time
Lactobacillus murins DSM 28683 *Lactobacillus paracasei* DSM 28675	De Man, Rogosa and Sharpe agar medium (MRS), (Liofilchem Diagnostic, Italy), 3 % (w/v) MRS and 1.5 % (w/v) agar microaerophilic 37°C	1-2 days
Acutalibacter muris DSM 26090 *Muribaculum intestinale* DSM 28989 *Faecalibaculum rodentium* DSM 103405	Columbia Blood Agar Base medium (CBA), (Liofilchem Diagnostic, Italy), supplemented with 5% defibrillated horse blood (Thermo Scientific, UK) anaerobic 37°C	3-7 days
Bacteroides dorei DSM 17855 *Clostridium cocleatum* DSM 1551 *Clostridioides mangenotii* DSM 29133 *Anaerotruncs colihominis* DSM 28734 *Clostridium beijerinckii* DSM 791	Columbia Blood Agar Base medium anaerobic 37°C	2-3 days
Bacteroides caecimuris DSM 26085	Columbia Blood Agar Base medium Anaerobic 37°C	1-2 days
Citrobacter freundii ATCC 8090	Tryptic Soy Agar (TSA) (Liofilmchem Diagnostic, Italy), (3 % (w/v) TSB and 1.5 % (w/v) agar) aerobic 37°C	1 day
Helicobacter pylori ATCC 700392 / 26695	Columbia Blood Agar Base medium microaerophilic 37°C	3 days

3.3 Optimization of hybridization conditions

3.3.1 LNA/2'OMe-FISH method

A universal LNA/2'OMe probe EUB338 (5'-mT*lG*mC*mC*lT*mC*mC*lC*mG*mT *lA*mG* mG*l A*-3') (Eurogentec, Belgium) based on Amann et al., (1990), specific for the Eubacteria domain, was used during the FISH experiments. LNAs (represented by "l") were placed at every third 2'OMe (represented by "m") monomer. The LNA/2'OMe probe EUB338 also included a phosphorothioate backbone (PS linkage represented by "*") instead of a phosphodiester.

The EUB338 probe targets a conserved region of the bacterial 16S rRNA which is predicted to be present in most bacteria and was verified to be present in microorganisms of this project.

In order to choose the best hybridization conditions for the group of microorganisms used in this work, 5 hybridization solutions were tested according Azevedo et al., (2018), which differ in their composition and therefore function at different hybridization temperature. Furthermore, in this experiment the LNA/2'OMe probe EUB338 were conjugated to its 5' end ATTO 550 fluorochrome.

First, the bacterial cells were harvested from MRS (*L. murinus*), TSA (*C. freundii*) and CBA plates supplemented with 5% defibrillated horse blood (*M. intestinale*, *F. rodentium*, *A. colihominis*, *C. beijerinkii*, *B. dorei* and *H. pylori)* and suspended in sterile water. Cell concentration was assessed by optical density (OD) at 620 nm and the suspension was diluted in order to obtain a final OD of 0.5. Then, for sample fixation/permeabilization, cell suspensions were centrifuged (10 000 x g, 5 min) and fixed in 400 µL of 4% (w/v) paraformaldehyde (Sigma, USA) for 1 hour at room temperature. After centrifugation, the fixed cells were resuspended in 500 µL of 50% (v/v) ethanol and incubated at -20°C for at least 30 min.

For hybridization, 100 µL of the fixed cells were pelleted by centrifugation (10 000 x g, 5 min) and resuspended in 100 µL of hybridization solution (Table 3.2) containing 200 nM of LNA/2'OMe probe EUB338. A control test similar to the one described above was performed with hybridization solution without the probe. This assessment is important to confirm that the positive results obtained are due to the probe hybridization. Samples were incubated during 60 min at the hybridization temperature (Table 3.2).

Table 3.2. Hybridization conditions tested with different denaturant reagents: urea, formamide and ethylene carbonate

	Hybridization Solution	Temperature
A	2M Urea (National Diagnostics, USA); 4M NaCl (Fisher Scientific, Belgium); 50 mM Tris-Hcl (pH 7.5) (Sigma, USA)	62 ºC
B	3M NaCl; 30% Formamide (Across Organic, New Jersey, US); 10% dextran sulphate (Fisher Scientific, US); 50 mM Tris-HCl (pH 7.5)	66 ºC
C	900 mM NaCl; 30% Formamide; 5 mM EDTA (Panrea, Spanish); 0.1% TritonX-100 (Sigma, USA); 50 nM Tris-HCl (pH 7.5)	66 ºC
D	5% Ethylene carbonate (Sigma Aldrich, Germany); 3 M NaCl; 50 mM Tris-HCl (pH 7.5)	62 ºC
E	1 M Urea; 4 M NaCl; 50 mM Tris-HCl (pH 7.5)	62 ºC

Afterwards, samples were centrifuged (10 000 x g, 5 min), resuspended in 500 µL of washing solution containing 5 mM Tris-base (pH 10; Sigma, USA), 15 mM NaCl (Fisher Scientific, Belgium) and 0.1% (v/v) Triton X-100 (Sigma, USA) and incubated for 30 min at

the same temperature used in the hybridization step. Finally, the suspension was pelleted by centrifugation (10 000 x g, 5 min) and resuspended in 500 µL of 0.9% (w/v) distilled water (Fisher Scientific, Belgium). Afterwards, for bacteria disaggregation some samples were subjected to sonication step by ultrasounds (Transsonic 420, Elma, Germany); *H. pylori* and *M. intestinale* were sonicated for 17 min; *B. dorei*, *B. caecimuris* and *F. rodentium* for 12 min.

The slides were coated with 0.01 % (w/v) of poly-L-lysine (Sigma, USA), for a better attachment of specimens to glass slides (Colville et al., 2010). After a 5 minutes incubation, the excess solution was removed, and the slides were dried at room temperature. Then, 10 µL of the cell suspension was put on a microscope slide coated with poly-L-lysine and allowed to air dry in a dark place or protected from light. Finally, the samples were mounted with one drop on non-fluorescent immersion oil (Merck, Germany) and visualized using a Leica DM LB2 epifluorescence microscope (Leica Microsystems GmbH, Germany) equipped with Leica DFC300 FX camera (Leica Microsystems GmbHy, Germany) and filter capable of detecting the LNA/2'OMe probe EUB338 attached to ATTO 550 (BP 514-560, FT 580, LP 590). For image capture, Leica Application Suite (LAS v4.2), was used.

3.4 Optimization of the Spectral Imaging-FISH using an LNA/2'OMe probe EUB338

3.4.1 Establishment of the bacterial species and fluorochromes rankings

For a successful Spectral Imaging-FISH, a balanced species/fluorochromes pairs should be establised in order to have an unambiguous separation of the fluorochromes in a multiplex assay. Hence, 8 versions of the LNA/2'OMe probe EUB338 attached to a different fluorochrome (Alexa Fluor 405, Alexa Fluor 488, Alexa Fluor 514, ATTO 532, ATTO 550, Alexa Fluor 594, ATTO 633 and ATTO 655) were used to rank the fluorochromes. These probes were used to label separate aliquots of *E. coli* cells in FISH reactions (Figure 3.1) according the protocol described in section 3.3.1.

For ranking of the bacteria, an LNA/2'OMe probe coupled with ATTO 550 were used to label separate aliquots of *L. murinus*, *L. paracasei*, *M. intestinale, F. rodentium, A. colihominis, C. cocleatum, C. mangenotii, C. beijerinckii, B. caecimuris, B. dorei, H. pylori and C. freundii* in FISH reactions (section 3.3.1. LNA/2'OMe-FISH method).

After FISH protocol, the samples were mounted with Fluoromount Mounting Medium (Sigma-Aldrich, USA) and the coverslips were placed. Then, the slides were let at room

temperature in the dark for 45 min. Finally, the samples were stored ate 4 ºC in the dark before confocal microscope analysis. All experiments were performed in duplicate.

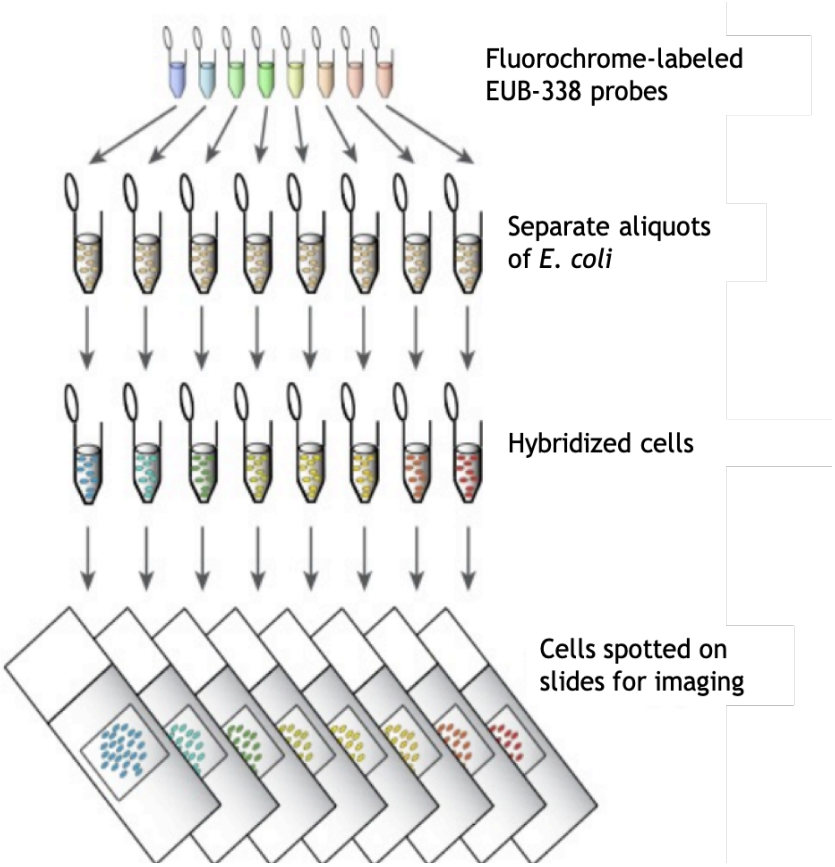

Figure 3.1. Eight different versions of LNA/2'OME probe (EUB338) attached to a different fluorochrome were used to label separate aliquots of *E. coli* in FISH reactions. Reprinted from Valm et al., (2012b).

3.4.2 Confocal microscope visualization and intensity fluorescence quantification

Samples were imaged with system Leica TCS SP5 II (Leica Microsystems, Germany), Inverted Microscope Leica DMI6000-CS (Leica Microsystems, Germany) equipped with a Diode 405, Argon 488, Argon 514, Argon 561 and HeNe 633 lasers.

The software used to capture the images was the LAS AF (Leica Microsystems, Germany) and the mode of acquisition used was: xyz. Images were acquired with the same settings with the HC PL APO CS 63 x /1.3 glycerol objective. Laser power was optimized for each fluorochrome assigned to each target to maximize signals without saturations

The fluorescence intensity of each image was quantified using the Fiji software (Wayne Rasband National Institutes of Health), according Appendix 2.

The fluorescence intensities provided by Fiji software were normalized using the equation i:

$$X' = \frac{X}{X_{máx}} \qquad \text{(equation i)}$$

Where X corresponds to the value to be normalized, while $X_{máx}$ is the maximum intensity value observed for the outputs.

3.5 Imaging Proof of Principle

3.5.1 Validation of method imaging and analysis

After LNA/2'OMe-FISH method (section 3.3.1), all of the labeled *E. coli* cells aliquots were then combined into a single tube to create a mixture of the 8 different fluorochromes Figure 3.2.

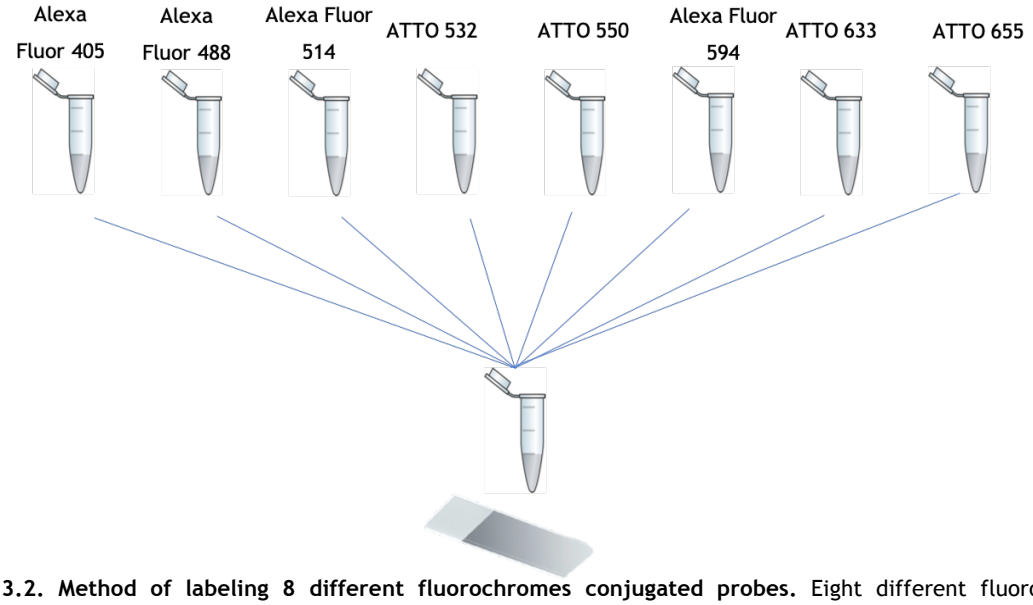

Figure 3.2. Method of labeling 8 different fluorochromes conjugated probes. Eight different fluorochrome-conjugated probes were used to label 7 separate aliquots of *E. coli* such that each aliquot received a unique fluorochrome. After FISH, all of the labeled *E. coli* aliquots were combined into a single tube to create a mixture. This mixture was then spotted on a slide for imaging.

Afterwards, to confirm the method ability to correctly distinguish the different relative proportions of bacteria, the same principle was applied to the mouse gastric bacterial species species (*Lactobacillus* sp., *Bacteroides* sp., *Clostridiales*, *M. intestinale* and *F. rodentium*), and also the *H. pylori* and *C. freundii*, with 7 fluorochromes coupled to these bacteria. The mixture was made an equal proportion, in which all label types are added in an equal amount. The Individual hybridizations were used to obtain the reference spectra and to count the frequency of each bacterium added in mixture.

Then the samples were placed on the slides according to the procedure outlined in section 3.4.1., and images were acquired and analyzed according procedure in section 3.5.2 and section 3.5.3, respectively.

3.5.2 Image Acquisition

Specimens were imaged with the same system mentioned above, in section 3.4.2. The software used to capture the images was the LAS AF (Leica Microsystems, Germany) and the mode of acquisition used was Live Data Mode, Acquisition mode: XYλ. Images were acquired with the same settings with HC PL APO CS 63 x /1.3 glycerol objective. For each laser line was used a specific laser power as shown in Figure 3.3, as well as detection begin and detection end, Table 3.3.

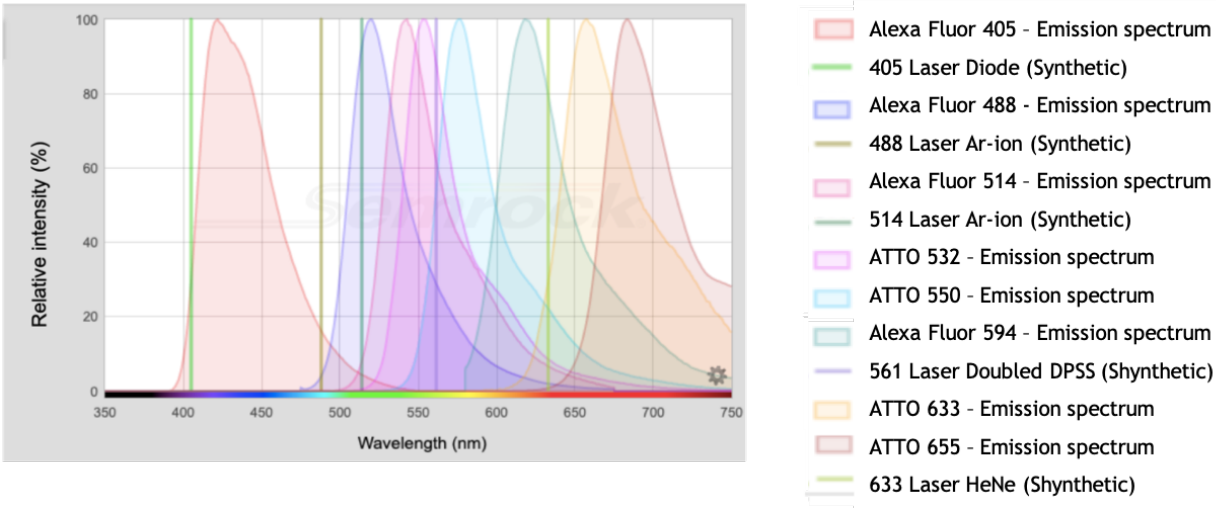

Figure 3.3. Emission spectra of each fluorochrome and lasers. Each laser line available on the microscope system, can detect different fluorochromes.

Firstly, to assign to each pixel in the image its fluorochrome, the linear unmixing algorithm requires, as input, the known reference spectra for all the fluorochromes used in an experiment. For this:

1) The best possible image of Alexa Fluor 405 with 405 nm excitation, Alexa Fluor 514, ATTO 532 and ATTO 550 with 514 wavelength excitation, ATTO 532, ATTO 550 and Alexa Fluor 594 with 561 wavelength excitation and Alexa Fluor 594, ATTO 633 and ATTO 655 with 633 wavelength excitations were acquired.
2) It was used the microscope confocal instrument software (LAS AF) to define a region of interest (ROI) in each cell in each image. Then the software calculated the average intensity over all the pixels in the ROI to generate a reference spectrum.

Reference spectrum specimens should be treated exactly as unknown microbial specimens.

For mixture of different fluorochromes, four spectral images acquisitions were made sequentially for each field of view in order of descending excitation wavelength, 633 nm, 561 nm, 514 nm and 405 nm, Table 3.3. In addition, individual images of 5 mouse gastric bacterial species, *H. pylori* and *C. freundii* labeled with a single fluorochrome were also acquired in order to be counted.

Table 3.3. Parameters used for the spectral image acquisition. For each laser line available on the microscope system, laser power was defined as well the detection begin and detection end

Sequential Analysis	Laser	Laser Power	Detection Begin – Detection End	Fluorochromes
1	633	30%	645 nm -700 nm	ATTO 633 ATTO 655
2	561	25%	571 nm -700 nm	ATTO 550 Alexa Fluor 594
3	514	25%	529 nm -700 nm	Alexa Fluor 514 ATTO 532
4	405	20%	416 nm -700 nm	Alexa Fluor 405

3.5.3 Image Analysis

Once a spectral image is recorded, it is necessary identify at each pixel of the image the fluorochrome composition. Hence, the linear unmixing algorithm available on the confocal software, was applied to recorded spectral images using reference spectra to generate multichannel images, in which, each channel consists of measured intensities assigned to one of the distinct fluorochromes used (Appendix 3). As multiple excitation wavelength was used sequentially to excite all the fluorochromes, then each excitation was unmixed separately. All of the reference spectra for fluorochromes maximally excited by a particular wavelength were used for unmixing that spectral data set. In addition, it was also necessary to include additional reference spectra which are more efficiently excited at other wavelengths, but which nonetheless are somewhat excited by the wavelength used in the imaging regime. Spectral images were converted to TIFF format in Fiji software and analyzed according Appendix 4.

Subsequently for the mixture an equal proportions (with mouse gastric bacterial species, *H. pylori* and *C. freundii*) the frequency of each label-type in individual images and

mixtures were counted. For individual images and mixtures were counted 6 images of each different bacteria.

3.6 Design and theoretical evaluation of LNA/2'OMe probes

3.6.1 Probe design

In this section it was intended to the design specific NAMs probes that will target rRNA regions of *Lactobacillus* sp., *M. intestinale*, *F. rodentium*, *Bacteroides* sp., Clostridiales, *H. pylori* and *C. freundii*.

The reported sequences for *Lactobacillus sp.*, Clostridiales, *Bacteroides sp.* and *H. pylori* were re-evaluated.

For other species, the 16S rRNA gene sequence of *M. intestinale*, *F. rodentium* and *C. freundii,* available at the ARB Silva database website (https://www.arb-silva.de/search/), were used to design the probes at PRIMROSE program. For that, only target sequences with >1200 bp, with high sequence quality, high alignment quality and high pintail quality, were used. Then, for identify the specie of interest it was select the Specify Target Taxon. Subsequent, it was intended identify all possible oligonucleotides that could target the taxon of interest. Finally, next step was to screen the oligonucleotide collection to identify which oligonucleotides best designate our taxon whilst excluding non-target sequences. These included no self-complementary structures within the probe and high specificity and sensitivity for microorganisms. The evaluation of self-complementary probes was performed with Applied Biosystems (http://www6.appliedbiosystems.com/support/pnadesigner.cfm). Once the probes sequence was selected, a search was made at the ARB Silva to further confirm probe specificity and sensitivity.

The type of NAMs for the design of probes was selected based on previous studies, which have demonstrate that LNA/2'OME benefits from great design flexibility, allowing different probes to operate with similar thermodynamic parameters such as melting temperature (Azevedo et al., 2015; Fontenete et al., 2016).

3.6.2 *In Silico* Evaluation of the probes

The determination of the theoretical specificity was based on equation ii:

$$specificity = \frac{nPs}{tPs} \times 100 \qquad \text{(equation ii)}$$

Where nPs stands for the total number of non-target strains that did not react with the probe and tPS is the total non-target strains examined.

The determination of the theoretical sensitivity was based on equation iii:

$$sensitivity = \frac{sS}{TSs} \times 100 \qquad \text{(equation iii)}$$

Where sS stands for the number of bacteria strains detected by the probe and TSs is the total number of bacteria strains present in the databases.

Besides specificity and sensitivity, other criteria for selection of the probe sequences were considered:

Probe length: Since both specificity and the hybridization temperature and time are partly dependent on probe length; this parameter is critical for the successful hybridization in FISH. Probes typically have 15-30 nucleotides in length. If the probe is too long, selectivity toward the target decrease, conversely probes with few bp in length wiil lack specificity (Yilmaz & Noguera, 2004).

Overall gibbs free energy (ΔG °) is a thermodynamic parameter that can be used as indicator of whether a reaction is thermodynamically favorable or not. A negative ΔG° value (ΔG° <0) is an indicator of a thermodynamically favorable reaction. ΔG ° should be lower than -13 kcal/mol of DNA probes to maximize hybridization efficiency without compromising specificity (Yilmaz & Noguera 2004). However, for LNA/2'OMe probes there is no information about the recommended threshold ΔG °. The introduction of LNA monomers increase the target affinity and consequently having a positive and additive effect on the Tm (Azevedo et al. 2015).

Pyrimidine content (GC) provides information about the strength of hybridization. GC of the probe should be around 60% (Giesen et al. 1998).

Absence of self-complementary structures, because sequences with inverse repeats, palindromes and hairpins in the sequence tend to aggregate (Cohn & Moldave, 1996).

Melting temperature (Tm) is defined as the temperature in which 50 % of the nucleic acids DNA stands are in the helix state and the other 50 % in the single stranded (Muro 2005). The optimal Tm for nucleic acid probes in the range 52-58 °C, usually provide better results than probes with lower Tm.in multiplex approaches, all different probes should be similar Tm; hence Tms were adjusted with the introduction of LNA and 2'OMe mimics in different positions of the probes (Abd-Elsalam 2003).

The melting temperature as well as the Gibbs free energy ΔG ° for each probe were predicted using a calculator generated by the research group.

4 Results and Discussion

The FISH approach has been shown to be a valuable technique to discriminate and to analyze the spatial distribution of the individual species *in situ* without disturbing the biofilm structure (Azeredo et al. 2017; Azevedo et al. 2015). However, an important limitation of FISH techniques is the low multiplex capability which is mainly related with (1) the number of distinguishable targets and (2) the difficulty of having probes working perfectly at the same hybridization conditions (Moter and Göbel 2000). Regarding the limited number of targets (1), this is due to the use of filters in fluorescence image acquisition which limits 2 or 3 color channels the number of fluorochromes that can be simultaneously differentiated. To address this issue, new approaches based on spectral imaging, are emerging. In these approaches, instead of looking to the colors being emitted by the sample, the spectral composition (spectrum shape) of each pixel is recorded. That spectrum will then be matched to a reference library to attribute the final composition of the image (Valm, Mark Welch, and Borisy 2012b). For dealing with the probes hybridization conditions (2), the team research, where this study was performed, has been using NAMs, such as, LNA and 2'OMe on FISH (Cerqueira et al. 2008; Azevedo et al. 2018).

Hence, considering the high potential of spectral imaging and the enhanced properties of NAMs, it is intended to combine these strategies to develop a new FISH methodology that allows a multiplexed and robust characterization of the gastric microbiota associated with the presence of *H. pylori* and *C. freundii*.

The choice of the fluorochromes is especially important in multiplex studies; hence, in this study, fluorochromes with excitation/emission profiles that allow them to be easily separated by spectral imaging, were used (Appendix 5: Table A1, Figure 3.3).

4.1 Selection of the hybridization condition for the Universal Eubacteria LNA/2'OMe probe EUB338

In the first stage of this work it was necessary to choose the best hybridization conditions for the bacteria of this study. Thus, different hybridization solutions that contains different denaturants agents such as urea, formamide and ethylene carbonate (Table 3.2), were tested. These conditions were selected based on an earlier study by the research group for LNA/2'OMe-FISH technique (Azevedo et al., 2018).

The results demonstrated that a good fluorescence intensity was obtained, for hybridization solution A and E which contains urea and hybridization solution B and C which contains formamide. The hybridization solution which contains ethylene carbonate (D) provided fluorescence intensities weaker in comparison with the other denaturant agents, Table 4.1 As expected, control experiments (without probe) do not showed levels of fluorescence, which means that our samples do not present autofluorescence.

Table 4.1 Comparison of the signal of hybridization solutions that contains different denaturants agents (urea, formamide and ethylene carbonate)

Microorganisms	Hybridization Solution				
	A	B	C	D	E
L. murins	+++	+++	+	++	+++
M. intestinale	++	+++	++	+	++
F. rodentium	++	++	++	++	+++
A. colihominis	+++	+++	+++	++	++
C. beijerinckii	+++	++	++	++	+++
B. *dorei*	+++	+++	+++	+	+++
H. pylori	+++	+++	+++	++	+
C. freundii	+	+	+++	++	+++

+++ excellent signal, ++ good signal, + weak
A, B, C, D and E described in Table 3.2

In fact, urea, formamide and ethylene carbonate are suitable denaturants for LNA/2'OMe-FISH applications (Azevedo et al. 2018).

One of the components of the hybridization solutions is formamide that performances as a denaturant or destabilizing agent allowing the hybridization to be carried out at lower temperatures. In this study, hybridization solutions consist of 30% formamide, and provides a good fluorescence intensity (Table 4.1B and C). However, *in vivo* experiments it is not possible to use formamide due to its toxic nature to human cells (Fontenete et al. 2013). While most diagnostic FISH protocols contain formamide to affect the binding affinity of the probes, hybridization buffers based on sodium chloride (NaCl) and urea without toxic formamide have also been applied efficaciously, as well as ethylene carbonate (Frickmann et al. 2017; Azevedo et al. 2018, 2015).

Ethylene carbonate it is non-toxic component and studies showed that presented major advantages compared to a formamide buffer (Matthiesen and Hansen 2012). In present study, this is not verified, despite the signal intensities using the ethylene carbonate buffer were still considerably good (Table 4.1D), the intensities were stronger using formamide buffer (Table 4.1B and C.).

However, in the present study the hybridization solution with urea is as an appropriate non-toxic alternative and provides good fluorescence intensities among the different bacteria as shown in Table 4.1A and E. Despite this, this data were corroborated by previous studies (Azevedo et al. 2018; Fontenete et al. 2013).

According Azevedo et al., (2018), when urea was applied to the LNA/2'OMe-FISH protocol, the ranges of optimal urea concentration are overlapped, which might simply the detection of several bacteria in a single experiment. Thus, the use of urea as a denaturant agent seem to be an adequate choice to balance the fluorescence signal among species and to reach a universal hybridization solution in multiplex assays (Azevedo et al., 2018).

For instance, other components, employed in the hybridization solutions, such as dextran sulphate and TritonX-100 will have to be substituted or have their concentrations decreased due to their toxicity. Dextran sulphate is used as an hybridization rate accelerator (Gerstein 2001), while TritonX-100 acts as a detergent and prevents non-specific binding. A balance in the concentration of these reagent simultaneously with the concentration of added formamide that will ensure reasonable kinetics and specificity of hybridization while keeping acceptable levels of toxicity (Fontenete et al. 2013).

Despite these similarities of fluorescence intensities between the various hybridization solutions, a hybridization solution with 2 M of urea and 4 M of NaCl, should be use in initial optimization of new LNA/2'OMe-FISH experiments, according Azevedo et al., (2018). Therefore, for this reason this was the hybridization solution selected for the next assays.

4.2 Optimization of the Spectral Imaging-FISH using an LNA/2'OMe probe EUB338

4.2.1 Ranking of Bacteria and Fluorochromes

The success of the FISH technique depends on the ability of the fluorescently labeled probe to access the rRNA of the targets organisms. Cells of different species have different ribosome contents between 10^3 and 10^5 ribosomes per cell (Micahel et al 2001). The amount of rRNA per cell is different according to the type of species and the metabolic state of the bacterial cell (Klappenbach et al., 2000). In fact, low fluorescence ratio in hybridized cells may be related with different factors, such as low ribosomal content of cells, difficulty in permeating cells and low accessibility of targets located in the rRNA (Amann et al., 1995; Yilmaz & Noguera, 2004). Because of this, discrepant fluorescence signals between different bacteria, with different characteristics and properties, could be observed. Hence, the fluorescence intensity of the different bacterial species used in this study was evaluated using an LNA/2'OMe

probe EUB338 couple to ATTO 550. The universal EUB338 probe is a useful probe to understand the interplay of FISH variables, with no influence of the target and probe sequence.

According Table 4.2, *F. rodentium* had better fluorescence intensities whereas *H. pylori* had worse fluorescence intensities. After quantification of the fluorescence intensity a ranking of bacteria was created, Table 4.2.

Table 4.2. Ranking of Bacteria, where *F. rodentium* exhibits higher fluorescence intensity whereas *H. pylori* exhibits the least fluorescence intensity

	Species	***Normalized fluorescence intensity***
F. rodentium	*Faecalibaculum rodentium*	1.000±0.003
C. freundii	*Citrobacter freundii*	0.722±0.044
Lactobacillus sp.	*Lactobacillus murinus*	0.809±0.011
	Lactobacillus paracasei	0.739±0.043
Bacteroides sp.	*Bacteroides caecimuris*	0.647±0.019
	Bacteroides dorei	0.584±0.001
Clostridiales	*Acutalibacter muris*	0.441±0.006
	Anaerotruncos colihominis	0.516±0.014
	Clostridioides mangenotii	0.783±0.007
	Clostridium beijerinckii	0.631±0.020
	Clostridium innocuum	0.831±0.031
	Clostridium sporogenes	0.954±0.033
M. intestinale	*Muribaculum intestinale*	0.430±0.007
H. pylori	*Helicobacter pylori*	0.338±0.008

Concerning the fluorochromes, the use of different fluorochrome can influence the yield of the hybridization (Bouvier and Del Giorgio 2003). In fact, the brightness of the fluorochrome will depend on its ability to absorb light and the efficiency at which the absorbed light is converted into emitted light. The absorbed wavelengths, energy transfer efficiency and time before emission depend on both the structure of the fluorochrome and its chemical environment (Moter and Göbel 2000). Fluorochromes with high quantum yields and molar extension coefficient (ε), have been preferred to overcome some problems related with low fluorescence intensity and sensitivity pH. These types of fluorochromes have significant higher staining and are more resistant to photobleaching (Wessendorf and Brelje 1992). The photobleaching of fluorochromes on exposure to high-intensity excitation light leads to the degradation of the fluorochromes and progressively reduces image brightness (Aitken et al., 2008; James, 2006). Furthermore, scattering of the intense, excitation light, which can

interfere with the dim fluorescence image, is minimized with a longer stokes shift (separation between the wavelengths corresponding to the excitation and emission maxima (Johnson 2005).

Table 4.3 shows the values of the molar extinction coefficient, quantum yield and brightness intensity for the fluorochromes of this study.

Table 4.3 Properties of Alexa Fluor 405, Alexa Fluor 488, Alexa Fluor 514, ATTO 532, ATTO 550, Alexa Fluor 594, ATTO 633 and ATTO 655 fluorochromes in terms of molar extinction coefficient (ε), quantum yield and brightness intensity. Adapted from: ("Fluorochromes Brightness Chart,"; "Properties of ATTO-Dyes,")

Flurochrome	ε ($cm^{-1}M^{-1}$)	Quantum yield	Brightness intensity
Alexa Fluor 405	34000	-	-
Alexa Fluor 488	71000	0.94	66740
Alexa Fluor 514	80000	-	-
ATTO 532	81000	0.80	59250
ATTO 550	120000	0.80	96000
Alexa Fluor 594	73000	0.64	46720
ATTO 633	130000	0.64	83200
ATTO 655	160000	0.30	48000

Hence, to rank the fluorochromes, 8 versions of the LNA/2'OMe probe EUB338 coupled to a different fluorochrome were used to label separate aliquots of *E. coli* in FISH reactions.

The ranking of fluorochromes is present in Table 4.4. Thus, for Leica TCS SP5 confocal microscope, ATTO 550 is the fluorochrome which exhibits the highest fluorescence intensity and the Alexa Fluor 488 has a lower fluorescence intensity.

Table 4.4 Ranking of Fluorochromes where ATTO 550 exhibits higher fluorescence intensity whereas Alexa Fluor 488 exhibits the least fluorescence intensity

Fluorochromes	Normalized fluorescence intensity
ATTO 550	1.000±0.000
ATTO 633	0.923±0.029
Alexa Fluor 514	0.761±0.062
Alexa Fluor 594	0.579±0.005
ATTO 532	0.468±0.005
Alexa Fluor 405	0.446±0.023
ATTO 655	0.293±0.022
Alexa Fluor 488	0.257±0.023

The fluorochrome Brightness Index Score is a relative indication of fluorescence intensity above the background for each fluorochrome conjugation. These values can differ

depending upon the flow cytometer, the instrument, laser power, buffer conditions, among other things. For this reason, exact rankings should be established for specific instrument (Lay 2009).

In conclusion, a strong variation on the fluorescence intensities was found between species and between fluorochromes, which were balanced by matching the bacteria displaying weaker fluorescence intensity species with the brightest fluorochromes and vice versa.

Then were match the 'weaker' species (*H. pylori*) with a 'stronger' fluorochrome (ATTO 550) and the 'stronger' species (*F. rodentium*) with 'weaker' fluorochrome (ATTO 655), as shown in Table 4.5.

Table 4.5. Attribution of Fluorochromes at each bacteria, the weaker species match with stronger fluorochromes and the stronger species match with weaker fluorochrome

Probe	Fluorochromes
Helicobacter pylori	ATTO 550
Muribaculum intestinale	ATTO 633
Clostridiales	Alexa Fluor 514
Bacteroides sp.	Alexa Fluor 594
Lactobacillus sp.	ATTO 532
Citrobacter freundii	Alexa Fluor 405
Faecalibaculum rodentium	ATTO 655

4.3 Imaging proof of Principle

4.3.1 Imaging Proof of Principle using *E. coli*

In conventional fluorescent microscopy, differentiation of probe conferred fluorescence has frequently hampered by the overlap of fluorescent wavelength that could be imaged though the same bandpass filter.

In our study, spectral imaging technology facilitated the detections of bacterial cells with fluorescently labeled probes with high overlapping.

Firstly, it was evaluated the utility of spectral images acquired at different excitation wavelengths by using same populations of *E. coli* as test object. Labeled *E. coli* make excellent test specimens for FISH and are useful for checking spectral image acquisition set-up. Thus, aliquots of *E. coli* were labeled in a fluorescence *in situ* hybridization experiment with different fluorochrome covalently conjugated to its 5' end of the same probe sequence, the LNA/2'OMe probe EUB338. The labelled cells were then combined to create a mixture of 8 different fluorochromes and were imaged and analyzed.

A disadvantage of multiple wavelength excitation and concatenation is related to time. Acquiring multiple images of the same field of view at different excitation wavelengths increase the time needed to image a specimen. This increase in time is not a significant problem for fixed samples but may cause problems for live cell imaging. Furthermore, fluorochrome bleaching is disadvantageous because it has the potential to reduce the signal to noise ratio in recorded images, but even more importantly for multiple wavelength concatenation, bleaching can impact artifacts in the excitation/emission profile of a fluorochrome.

After image analyses by linear unmixing algorithm and Fiji software the image shown in Figure 4.1 were obtained, with 8 distinct colors.

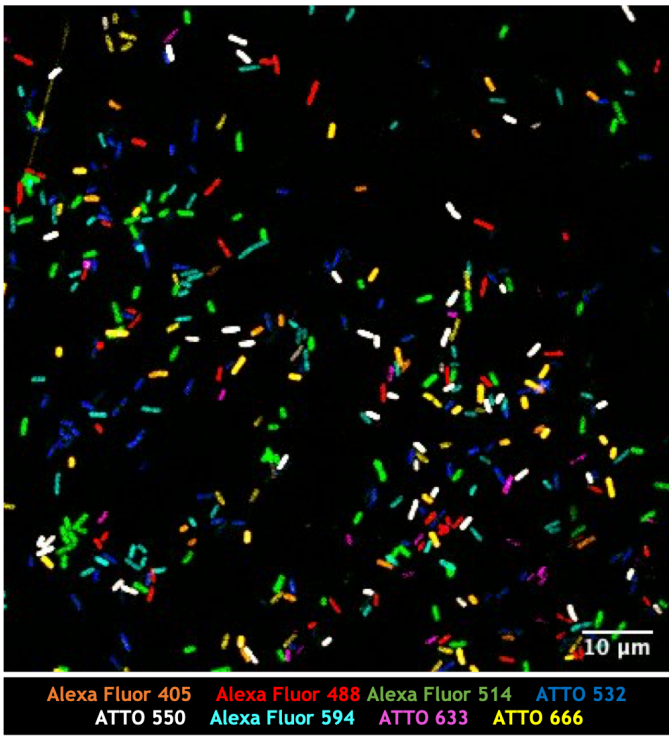

Figure 4.1. FISH proof of principle with *E. coli* labeled with 8 different fluorochromes after standard linear unmixing that concatenate spectral data from multiple spectral images of a single fields of view.

In fact, the results demonstrated in Figure 4.1, shown that using spectral imaging on Leica TCS SP5 Confocal, it was possible discriminate 8 fluorochromes, Alexa Fluor 405, Alexa Fluor 488, Alexa Fluor 514, ATTO 532, ATTO 550, Alexa Fluor 594, ATTO 633 and ATTO 655 in a multiplex assay.

These results confirm the accuracy of FISH and establish as proof of principle that a mixture of microbes labeled with different fluorochromes can be distinguished correctly in a single spectrally acquired image after linear unmixing.

To assess the accuracy of the assay, the same acquisition and image-processing protocols used to characterize the microbial mixture were applied to the preparations of the 7 bacteria used in this work, section 4.3.2.

4.3.2 Imaging Proof of Principle using mouse gastric bacterial species

In a natural community there are different bacterial species simultaneously present. In establishing biological proof of principle, we sought to demonstrate that different mouse gastric bacterial species (*L. paracasei*, *F. rodentium*, *M. intestinale*, *B. dorei* and *C. mangenotii*) and also *C. freundii* and *H. pylori* mixed after labeling, could be distinguished with an universal probe EUB 338 couple to their respective fluorochrome (Table 4.5) in FISH reactions.

To facilitate the definition of power and gain of each laser, it was done double mixtures corresponding to each sequential analysis. Then, spectral images were acquired sequentially with separate wavelength excitation and linear unmixing was applied to the spectral images giving rise to Figure 4.2.

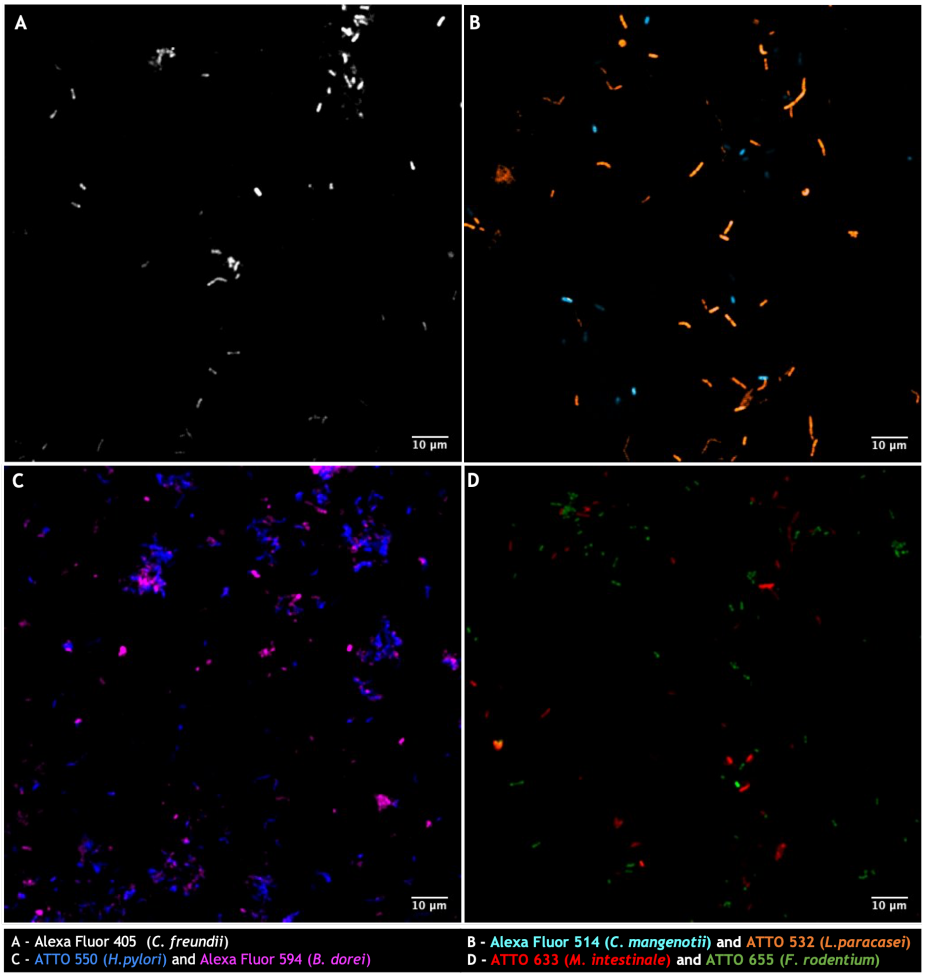

Figure 4.2. Mixtures for different sequential analyses. A. correspond to sequential analysis 4 and detects Alexa Fluor 405; B. correspond to sequential analysis 3 and detects Alexa Fluor 514 and ATTO 532; C. correspond to sequential analysis 2 and detects ATTO 550 and Alexa Fluor 594; D. correspond to sequential analysis 1 and detects ATTO 633 and ATTO 655.

For sequential analysis 4 (laser 405) that contains *C. freundii* couple to Alexa Fluor 405, the best laser power was defined to 20% (Figure 4.2.A). For sequential analysis 3 with laser 514, constituted by *L. paracasei* coupled to ATTO 532 and *C. mangenotii* coupled to Alexa Fluor 514 (Figure 4.2.B) the laser power was set to 25%. The same laser power value (25%) was set for

analyze sequence 2 (with laser 561) that contains *B. dorei* coupled to Alexa Fluor 594 and *H. pylori* coupled to ATTO 550 (Figure 4.3.C). Lastly, for laser 633 (sequential analysis 1), constituted by *M. intestinale* coupled to ATTO 633 and *F. rodentium* coupled to ATTO 655, laser power was set to 30%, Figure 4.4.D.

After these conditions were defined the 7 bacteria coupled to the different fluorochromes were then combined to create a mixture, in the same way as in section 4.3.1. Although some bacteria are aggregated, spectral imaging actually allows the separation of the different bacteria Figure 4.3.

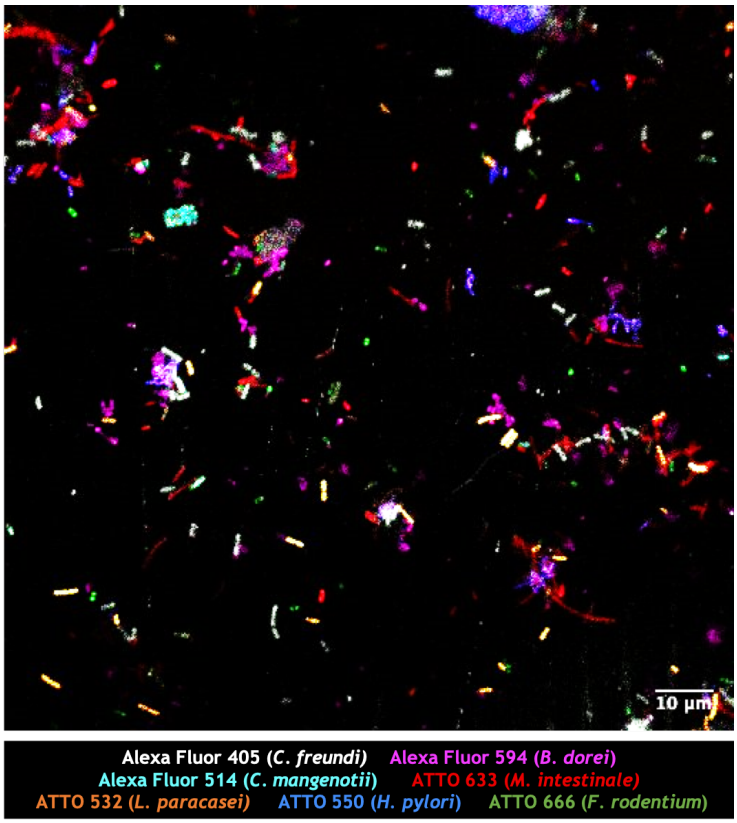

Figure 4.3. Mouse gastric bacterial species, *C. freundii* and *H. pylori* labeled with 7 different after standard linear unmixing that concatenates spectral data from multiple spectral images of a single fields of view.

In fact, in this proof-of-principle experiment, it was demonstrated a florescence imaging assay capable of distinguishing 7 different labeled microbes (*L. paracasei, M. intestinale, F. rodentium, B. dorei, C. mangenotii, H. pylori* and *C.freundii*) in a single field of view when imaged using a TCS SP5 confocal microscope with 4 lasers excitation wavelengths.

However, it was needed to verify if the bacteria are correctly imaged and unmixed using the set of image acquisition and analysis parameters here optimized. Hence, the frequency of each bacterium in the mixture must be equivalent to the frequency of each species in the individual images from our spectral imaging-FISH (Figure 4.4).

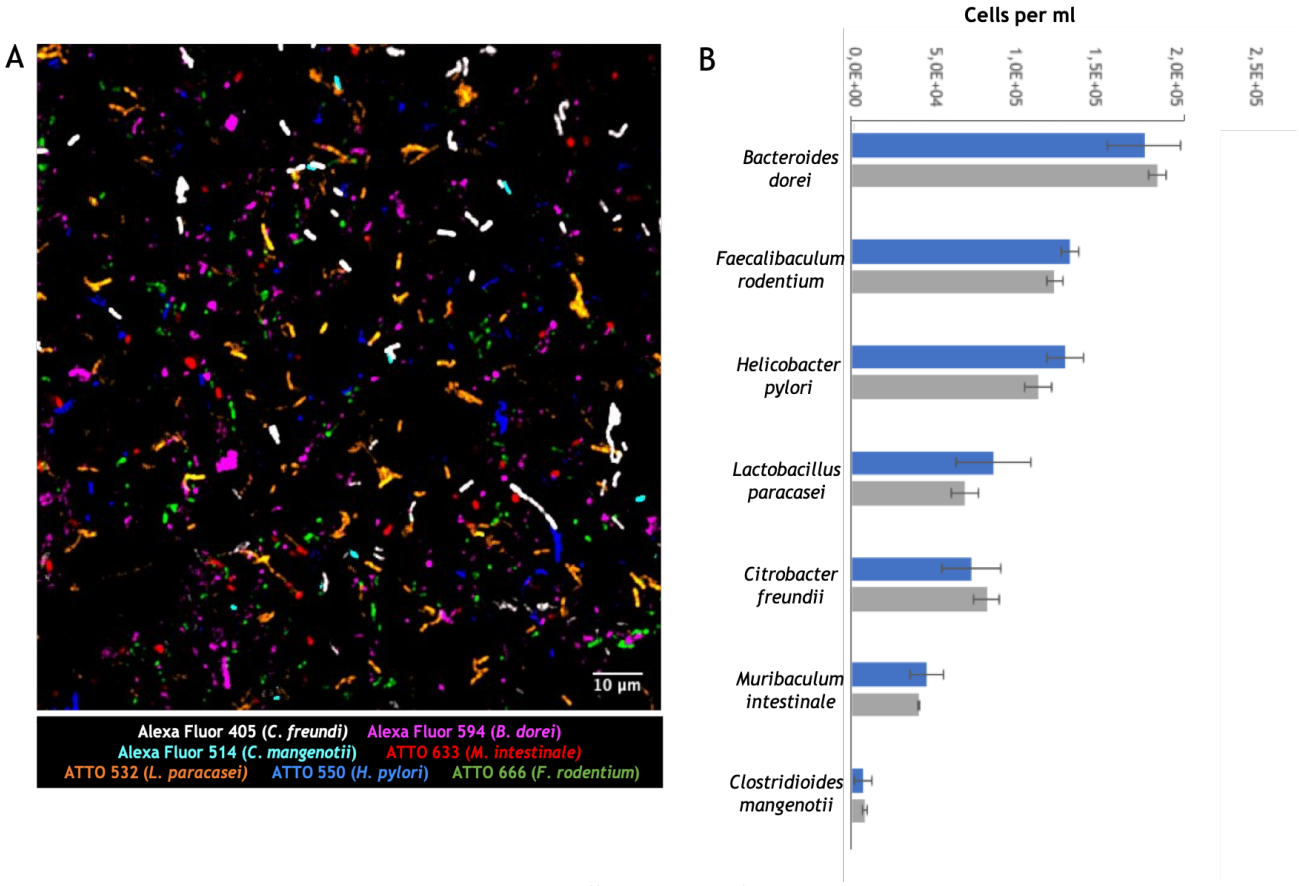

Figure 4.4. Mouse gastric bacterial species, *C. freundii* and *H. pylori* labeled with 7 different fluorochromes in equal proportion. In A. mixture may be an equal mixture, in which all label types are added in an equal amount after standard linear unmixing using an algorithm that concatenates spectral data from multiple spectral images of a single fields of view. In B. quantification of input into the mixture (gray bars) with output (blue bars). Error bars in input represent standard deviation in the count of cells from four different fields of view of a single-species preparation; error bars in the output measurements represent standard deviations of each species counted in six different fields of view of spectral imaging labeled microbes.

After linear unmixing (Appendix 3), image analyses (Appendix 4) and quantitative analysis, all differently labeled mouse gastric bacterial species, *C. freundii* and *H. pylori* were identified in the image and in approximately equal proportion as expected, Figure 4.4.B.

In fact, the separate spectral imaging it works since the frequency of each label type in individual images and mixtures are similar. In fact, this input into the mixture of mouse gastric bacterial species, *C. freundii* and *H. pylori*, correlated with output after image analysis, thereby establishing biological proof of principle of spectral imaging-FISH. Together, the results confirm the accuracy of Spectral Imaging–FISH and establish as proof of the principle using

mouse gastric bacterial species. Problems associated with autofluorescence were insignificant in our samples.

Overall, it was demonstrated an extraordinary ability to distinguish fluorochromes with highly overlapping emission spectra. This is a significant improvement in the number of fluorescent labels previously distinguished in conventionally microbial FISH and this method expand the number of distinguishable fluorescent reporters within a single image.

Typically, the systems level analysis of complex biological structures afforded by spectral imaging-FISH strategy offers an approach for study the biological organization of gastric microbiota. It is expected that this method combined with NAMs probes provides an accurate characterization of gastric microbiota. Therefore, future work will focus on imaging and unmixing of unknown gastric samples labeled with taxon-specific probes (probes designed in section 4.4).

4.4 *In Silico* Evaluation of the probes

The last task of this study was dedicated to the design of the taxon-specific NAMs probes that will target rRNA regions. Common species/ genus/ order present in gastric microbiota were selected as targets. The type of NAMs for the design of probes were selected based on previous studies, which have demonstrated that for FISH the use of LNA and 2'OMe would be advantageous (Azevedo et al. 2018).

The probes designed and re-evaluated are showed in Table 4.6.

Table 4.6. Sequences of LNA/2'OMe probes synthesized in this study, theoretical sensitivity, specificity, melting temperature, gibbs free energy

Target	Probe	Sequence (5'-3')	No. of targets in database	[a]No. of target strains detected	[a]No. of non-target strains detected	Specificity	Sensitivity	Tm (°C)	ΔG ° Kcal/ mol	Reference
H. pylori	specie	mAlGmAmCmTmAlAmGmClClCmTlCmC	887	850	13	99.99%	95.82%	77.40	-31.90	(Guimarães et al. 2007)
Bacteroides sp.	genus	lAmGlClCmGmCmAlAmAlCmTmTlTlC	1429	1333	157	99.99%	93.28%	77.46	-28.79	(Gordon 2015)
Clostridiales	ordem	lCmTlTlClCmTmClClGmTlTmTlTlG	1327	1103	157	99.99%	83.12%	77.48	-31.97	(Lücker et al. 2007)
Lactobacillus sp.	genus	lCmClAlCmClTlTmCmClTlCmClGmG	12837	11733	116363	97.80%	91.40%	77.17	-35.26	(Kwon et al. 2004)
M. intestinale	specie	mClCmClCmTmClGmGmClCmAmClAmT	1	1	1	99.99%	100.00%	77.58	-31.88	This study
F. rodentium	specie	mClTmClTlCmAmGmGlCmClGmGlCmT	3	3	1	99.99%	100.00%	77.41	-30.00	This study
C. freundii	specie	mClClAmGlTlTmTmClGlGmAlTlGmC	554	532	1385	99.97%	96.02%	77.58	-31.23	This study

LNA nucleotide monomers are represented with "l"; 2´OMe-RNA monomers are represented with "m".

[a] Calculated by the ARB silva program (last accession, May 2019).

According to the ARB Silva, theoretical sensitivities of 95.8%, 93.3%, 83,1%, 91.4%, 100%, 100% and 96% were obtained for *H. pylori, Bacteroides*. sp, Clostridiales*, Lactobacillus sp., M. intestinale, F. rodentium* and *C. freundii* probe, respectively. In addition, as shown in Table 4.6, all probes display high specificity (approximately 100%). The absence of cross-hybridization with the other species under study is the most important criteria, providing further evidence of its usefulness for gastric microbiota detection.

Relatively to probe for *H. pylori*, it also detects *Helicobacter acinonychis (*100%). Furthermore, the genus *Bacteroides* probe seems to detect additionally *Aureitalea marina (100%), Alloprevotella rava (72%), Cytophaga xylanolytica (54%), Algitalea ulvae (100%) and other bacteria in lower percentages*. For order Clostridiales probe, in additions to detecting Clostridiales, also detects mostly *Nitrosococcus oceani* (83%), *Xanthomonadales (80%)* and also other bacteria *in low percentages*. The *Lactobacillus* sp. probe detects mostly *Lactobacillus sp.*, however, also detects *Bacillus anthracis* (57%), *Streptococcus dysgalactiae* (98%), *Pseudomonas aeruginosa* (94%) and other bacteria in *low percentages*. Relatively for the probes that were designed in this study, the probes for *M. intestinale* detect only *Parabacteroides (100%)* and *F. rodentium* probe detect bacteria in *low percentages* in addition to the target bacteria. Lastly, the probe designed for *C. freundii* detects beyond the target other *Citrobacter (57.2%) and* some *Enterobacter and E. coli* in low percentages. Although these probes have detected non-target microorganisms, it is not critical because these bacteria are not a common bacteria from gastric microbiota.

Overall, the *in silico* analyses indicated that the probes are able to detect specifically each target species, with no cross-complementary observed with the other microorganisms used in this project.

Concerning, the melting temperatures, as the aim is to apply the probes under the same hybridization conditions in a multiplex assay, the Tms values should be similar; in fact, observing Table 4.6, it was possible to obtain a similar Tm values for all probes (~77.55 °C) intercalating of LNA nucleotides with or 2'OMe mimics.

Furthermore, the probe affinity is defined as ΔG°, and a threshold ΔG° of -13 kcal/mol has been suggested for the design of DNA probes to guarantee a good hybridization efficiency. However, for LNA/2'OMe probes there is no information about the recommended threshold ΔG°. In this study, values of ΔG° between -29 and -35 kcal/mol were obtained for LNA/2'OMe probes, which is in agreement with a recent work by Azevedo et al., (2015).

In reality, these are actually the first LNA/2'OMe probes specifically designed for Clostridiales*, Lactobacillus* sp., *Bacteroides* sp., *M. intestinale*, *F. rodentium* and *C. freundii* detection.

After that, these probes will be ordered and will be optimized though well-established FISH procedures.

5 Conclusions

The FISH method is a very powerful molecular technique for bacterial detection and quantification, both in environmental samples and in clinical samples. In fact, this technique has become increasingly powerful due to the appearance of NAMs, which replace the traditional DNA probes.

Concerning the optimization of the hybridization conditions of the FISH procedure, it was concluded that hybridization solution consisting of urea and high salt concentrations (2 M of urea and 4M of NaCl) and hybridization temperature of 62 ºC seem to be an adequate choice to balance the fluorescence signal among mouse gastric bacterial species, *H. pylori* and *C. freundii* coupled to an universal LNA/2'OMe probe with 14 bp. Despite this, this data were corroborated with an earlier study by our research group.

Furthermore, as FISH is usually limited to two or three microorganisms, the Spectral Imaging-FISH approach allows to expand the number of microorganisms that can be discriminated in a single sample. The results demonstrated that, using spectral imaging on Leica TCS SP5 Confocal, it was possible distinguish 8 fluorochromes (Alexa Fluor 405, Alexa Fluor 514, ATTO 532, ATTO 550, Alexa Fluor 594, ATTO 633 and ATTO 655) in a unique sample. In fact, the technique was validated for 5 mouse gastric bacterial species, *H. pylori* and *C. freundii*, once the output from the spectral imaging-FISH was correlates with the input into the mixture; the frequency of each label type was counted in individual images and mixtures are similar.

Sequence probes were also designed, and sequences were re-evaluated for mouse gastric bacterial species. Concerning the sequence probes available on literature for *H. pylori*, *Bacteroides* sp. and Clostridiales detection, they were re-evaluated and they presented a high specificity and sensitivity. For *M. intestinale*, *F. rodentium* and *C. freundii*, the LNA/2'OMe probes designed also presented high specificity and sensitivity. The remarkable properties of LNA and 2'OMe mimics allowed a control of the thermodynamic parameters by doing mixed synthesis (intercalation of LNA nucleotides with or 2'OMe mimics); thus, all probes have melting temperature of approximately 77.55 ºC, simplifying detection of multiple targets simultaneously.

Therefore, the FISH technique in combination with spectral imaging analysis offers great advantageous for the detail investigation of gastric microbiota communities and, in future, could be the key factor to improve therapeutic strategies to combat or prevent gastric diseases.

6 Assessment of the work done

6.1 Objectives Achieved

The main goal of this work was to implement the NAMs-Spectral Imaging-FISH in mouse gastric bacterial species, *H. pylori* and *C. freundii*. For this purpose, was necessary optimize the hybridization conditions for these microorganisms, thus the optimal hybridization solution and temperature were selected. After the optimum hybridization conditions were defined, the ranking of fluorochromes and bacteria were performed to match the bacteria displaying weaker fluorescence intensity with the brightest fluorochrome and vice-versa.

Furthermore, spectral imaging-FISH was applied efficiently to mouse gastric bacterial species and also *H. pylori* and *C. freundii* labeled with 7 different fluorochromes. Additionally, it was verified that input into the mixture of mouse gastric bacterial species, *C. freundii* and *H. pylori*, has correlated with output after image analysis, thereby establishing biological proof of principle of spectral imaging-FISH. Moreover, species-specific LNA/2'OMe probes were designed for *C. freundii, M, intestinale and F. rodentium,* whereas for *H. pylori*, *Lactobacillus* sp., *Bacteroides* sp. and Clostridiales sequences available on literature were re-evaluated. Thus, the objective for this work were achieved and the technique it was validated.

6.2 Other works carried out

Presentation of this project on 12th Meeting of Young Researchers of University of Porto in 13th-15th February 2019, Porto, Portugal.

Support in the elaboration of a presentation for Mathew Fields, director of the Center for Biofilm Engineering at Montana, USA, and Darla Goeres, Associate Research Professor from the same institution in 11th-12th June 2019, Porto, Portugal.

This work will be presented in XXXIInd Workshop of the European Helicobacter & Microbiota Study Group in 5th-7th September 2019, Innsbruck, Austria.

6.3 Limitations and future work

As with any methodology, spectral image and linear unmixing is affected by different parameters that need to be optimized for the best possible results. The amount of overlap of the contributing spectra influences how reliably different signals can be distinguished. In this work, the ATTO 532 and ATTO 550 in some assays they were not effectively discriminated; as such, in the future the probes coupled to these fluorochromes have to be optimized.

However, it is intended to test different proportions of each mouse gastric bacterial species to validate the spectral imaging-FISH in which different volume of each label-type is added to the mixture to give different relative proportions in the final mixture.

Furthermore, some bacteria of this project tend to form aggregates which made it difficult to count in the assay described in the results and discussion. Nevertheless, in future, this methodology will be applied in gastric biopsies whose bacteria are aggregated by nature. Cells from natural environments normally exhibits autofluorescence. In this case, a labeled specimen may be imaged using at the same parameters as labeled images. The spectra from autofluorescent cells are recorded and added to the fluorochrome library along with the all microorganisms reference spectra. Autofluorescence is thus treated as another spectral character in the labeled sample and may be easily identified after unmixing.

Moreover, the probes that were designed will be ordered and after that, the probes will be optimized through-well-established FISH procedures and evaluated in terms of experimental specificity and sensitivity. The experimental determination of the melting temperature will be determined, since the values obtained in this thesis are theoretical.

After optimization of all probes, the method will be validated and implemented in gastric biopsies of mouse models to assume their potential applications in *in vivo* studies. Some adjustments in protocol previously optimized in this work might be done in order to have a high signal-to-noise ratio in a multiplex experience.

Finally, as a case study, it is intended study of the gastric microbiota since the knowledge about the role and functions of gastric microbiome during *H. pylori*/ C. *freundii* infection is insufficient. This method will be useful to model the gastric microbiota changes in terms of localization and composition during *H. pylori* and *C. freundii* infection. This technique will allow to understand the relationship between gastric microbiota and *H. pylori* and *C. freundii*.

6.4 Final Assessment

Realization of this thesis in LEPABE gave me the opportunity to know what it is to actually work in research and in laboratory. Meeting working schedules, planning a day's work including the necessary materials, as well as coordinating with other people was a different reality from what I have lived so far. Despite this, it also gave me a lot of autonomy and experience in finding solutions rapidly. In addition, I also deepened my research skills and equipment handling to perform this project.

References

Abd-Elsalam KA. Bioinformatic tools and guideline for PCR primer design. 2003. doi: 10.5897/AJB2003.000-1019

Adamsson I, Nord CE, Lundquist P, Sjöstedt S, Edlund C. Comparative effects of omeprazole, amoxycillin plus metronidazole versus omeprazole, clarithromycin plus metronidazole on the oral, gastric and intestinal microflora in Helicobacter pylori-infected patients. J Antimicrob Chemother. 1999;44(5):629-640. doi: 10.1093/jac/44.5.629

Aitken CE, Marshall RA, Puglisi JD. An Oxygen Scavenging System for Improvement of Dye Stability in Single-Molecule Fluorescence Experiments. Biophys J. 2008;94(5):1826. doi:10.1529/BIOPHYSJ.107.117689

Alarcón T, Llorca L, Perez-Perez G. Impact of the Microbiota and Gastric Disease Development by Helicobacter pylori. In: Springer, Cham; 2017:253-275. doi:10.1007/978-3-319-50520-6_11

Almstrand R, Daims H, Persson F, Sörensson F, Hermansson M. New Methods for Analysis of Spatial Distribution and Coaggregation of Microbial Populations in Complex Biofilms. Appl Environ Microbiol. 2013;79(19):5978-5987. doi:10.1128/aem.01727-13

Amann R, Fuchs BM, Behrens S. The identification of microorganisms by fluorescence in situ hybridisation. Curr Opin Biotechnol. 2001;12(3):231-236. doi: 10.1016/S0958-1669(00)00204-4

Amann RI, Binder BJ, Olson RJ, Chisholm SW, Devereux R, Stahl DA. Combination of 16S rRNA-targeted oligonucleotide probes with flow cytometry for analyzing mixed microbial populations. *Appl Environ Microbiol*. 1990;56(6):1919-1925.

Amann R, Fuchs BM. Single-cell identification in microbial communities by improved fluorescence in situ hybridization techniques. *Nat Rev Microbiol*. 2008;6(5):339-348. doi:10.1038/nrmicro1888

Amann RI, Ludwig W, Schleifer K-H. *Phylogenetic Identification and In Situ Detection of Individual Microbial Cells without* Cultivation. Vol 59.; 1995

Andersen ML, Winter LMF. Animal models in biological and biomedical research - experimental and ethical concerns. *An Acad Bras Cienc*. 2017;91(suppl 1). doi:10.1590/0001-3765201720170238

Andersen ML, Winter LMF. Animal models in biological and biomedical research – experimental and ethical concerns. 2019:91. doi:10.1590/0001-3765201720170238

Atherton JC, Blaser MJ. Coadaptation of Helicobacter pylori and humans: ancient history, modern implications. *J Clin Invest*. 2009;119(9):2475-2487. doi:10.1172/JCI38605

Azeredo J, Azevedo NF, Briandet R, et al. Critical review on biofilm methods. *Crit Rev Microbiol*. 2017;43(3):313-351. doi:10.1080/1040841X.2016.1208146

Azevedo AS, Sousa IM, Fernandes R, Azevedo NF, Almeida C. Optimizing locked nucleic acid/2-O-methyl-RNA fluorescence in situ hybridization (LNA/2OMe-FISH) for bacterial detection. *CHEMPOR 2018 - 13th Int Chem Biol Eng Conf (b Ext Abstr*. 2018;(P-BB12):226-227. http://repositorium.sdum.uminho.pt/handle/1822/56854. Accessed March 16, 2019.

Azevedo AS, Almeida C, Pereira B, Madureira P, Wengel J. Detection and discrimination of biofilm populations using Locked Nucleic Acid/2'-O-Methyl-RNA Fluorescence In Situ Hybridization (LNA/2'OMe-FISH) 6. *Biochem Eng J*. 2015;104(1):64-73. doi:10.1016/j.bej.2015.04.024

Aviles-Jimenez F, Vazquez-Jimenez F, Medrano-Guzman R, Mantilla A, Torres J. Stomach microbiota composition varies between patients with non-atrophic gastritis and patients with intestinal type of gastric cancer. *Sci Rep*.

2015;4(1):4202. doi:10.1038/srep04202

Bauman JGJ, Wiegant J, Borst P, van Duijn P. A new method for fluorescence microscopical localization of specific DNA sequences by in situ hybridization of fluorochrome-labelled RNA. Exp Cell Res. 1980;128(2):485-490. doi:10.1016/0014-4827(80)90087-7

Bhatia U, Robison K, Gilbert W. Dealing with database explosion: a cautionary note. Science. 1997;276(5319):1724-1725. doi: 10.1126/science.276.5319.1724

Bik EM, Eckburg PB, Gill SR, et al. Molecular analysis of the bacterial microbiota in the human stomach. *Proc Natl Acad Sci*. 2006;103(3):732-737. doi:10.1073/pnas.0506655103

Bottari B, Ercolini D, Gatti M, Neviani E. Application of FISH technology for microbiological analysis: current state and prospects. *Appl Microbiol Biotechnol*. 2006;73(3):485-494. doi:10.1007/s00253-006-0615-z

Bouvier T, Del Giorgio PA. Factors influencing the detection of bacterial cells using fluorescence in situ hybridization (FISH): A quantitative review of published reports. *FEMS Microbiol Ecol*. 2003;44(1):3-15. doi:10.1016/S0168-6496(02)00461-0

Brawner KM, Morrow CD, Smith PD. Gastric microbiome and gastric cancer. Cancer J. 2014;20(3):211-216. doi: doi.org/10.1097/PPO.0000000000000043

Brown JF, Balish E. *Gastrointestinal Microecology of BALB/c Nude Mice*.; 1978.

Cao L, Yu J. Effect of Helicobacter pylori Infection on the Composition of Gastric Microbiota in the Development of Gastric Cancer. *Gastrointest tumors*. 2015;2(1):14-25. doi:10.1159/000380893

Cerqueira, Azevedo N, Almeida C, Jardim T, Keevil C, Vieira M. DNA Mimics for the Rapid Identification of Microorganisms by Fluorescence in situ Hybridization (FISH). *Int J Mol Sci*. 2008;9(10):1944-1960. doi:10.3390/ijms9101944

Cerqueira L, Fernandes RM, Ferreira RM, et al. Validation of a Fluorescence In Situ Hybridization Method Using Peptide Nucleic Acid Probes for Detection of Helicobacter pylori Clarithromycin Resistance in Gastric Biopsy Specimens. *J Clin Microbiol*. 2013;51(6):1887-1893. doi:10.1128/JCM.00302-13

Clemente JC, Ursell LK, Parfrey LW, Knight R. The Impact of the Gut Microbiota on Human Health: An Integrative View. *Cell*. 2012;148(6):1258-1270. doi:10.1016/j.cell.2012.01.035

Cohen S, Valm AM, Lippincott-Schwartz J. Multispectral Live-Cell Imaging. *Curr Protoc Cell Biol*. 2018;79(1):1-13. doi:10.1002/cpcb.46

Cohn EW, Moldave K. *Progress in Nucleic Acid Research and Molecular Biology - Google Livros*. https://books.google.pt/books?id=Kp87qbd1zTIC&pg=PA34&lpg=PA34&dq=sequences+with+inverted+repeats+and+hairpins+tend+to+aggregate&source=bl&ots=wXf4bzywmN&sig=ACfU3U28f34zviwg6annqt6fqIRb4uJp0A&hl=pt-PT&sa=X&ved=2ahUKEwjap7uKpMviAhWQ2hQKHWTUCiEQ6AEwDHoECAc. Accessed June 2, 2019.

Colville K, Tompkins N, Rutenberg AD, Jericho MH. Effects of Poly(l -lysine) Substrates on Attached *Escherichia coli* Bacteria. *Langmuir*. 2010;26(4):2639-2644. doi:10.1021/la902826n

Cotter PD, Hill C. Surviving the acid test: responses of gram-positive bacteria to low pH. *Microbiol Mol Biol Rev*. 2003;67(3):429-453, table of contents. doi:10.1128/mmbr.67.3.429-453.2003

Dejea CM, Wick EC, Hechenbleikner EM, et al. Microbiota organization is a distinct feature of proximal colorectal cancers. *Proc Natl Acad Sci*. 2014;111(51):18321-18326. doi:10.1073/pnas.1406199111

Delgado S, Cabrera-Rubio R, Mira A, Suárez A, Mayo B. Microbiological Survey of the Human Gastric Ecosystem Using Culturing and Pyrosequencing Methods. Microb Ecol. 2013;65(3):763-772. doi:10.1007/s00248-013-0192-5

DeLong EF, Wickham GS, Pace NR. Phylogenetic stains: ribosomal RNA-based probes for the identification of single cells. Science. doi: 10.1126/science.2466341

Dickinson, E. M, Hessling R, Davidnson, W. M. Practical Considerations for Specral Imaging. 2014:1-15.

Engstrand L, Lindberg M. Helicobacter pylori and the gastric microbiota. *Best Pract Res Clin Gastroenterol*. 2013;27(1):39-45. doi:10.1016/j.bpg.2013.03.016

Fan Y-S. *Molecular Cytogenetics : Protocols and Applications*. Humana Press; 2002. https://books.google.pt/books/about/Molecular_Cytogenetics.html?id=gdoUrDiPtN4C&redir_esc=y. Accessed March 21, 2019. Accessed March 2, 2019

Ferreira RM, Pereira-Marques J, Pinto-Ribeiro I, et al. Gastric microbial community profiling reveals a dysbiotic cancer-associated microbiota. *Gut*. 2018;67(2):226-236. doi:10.1136/gutjnl-2017-314205

Ferrer MD, Mira A. Oral Biofilm Architecture at the Microbial Scale. *Trends Microbiol*. 2016;24(4):246-248. doi:10.1016/j.tim.2016.02.013

Figueiredo C. Helicobacter pylori and Interleukin 1 Genotyping: An Opportunity to Identify High-Risk Individuals for Gastric Carcinoma. *CancerSpectrum Knowl Environ*. 2002;94(22):1680-1687. doi:10.1093/jnci/94.22.1680

Fluorochromes Brightness Chart. https://www.bu.edu/flow-cytometry/files/2013/06/Fluorochromes-Brightness-Chart.pdf. Accessed June 19, 2019.

Fontenete S, Guimarães N, Leite M, Figueiredo C, Wengel J, Filipe Azevedo N. Hybridization-Based Detection of Helicobacter pylori at Human Body Temperature Using Advanced Locked Nucleic Acid (LNA) Probes. Veedu RN, ed. *PLoS One*. 2013;8(11):e81230. doi:10.1371/journal.pone.0081230

Fontenete S, Leite M, Guimarães N, et al. Towards Fluorescence In Vivo Hybridization (FIVH) Detection of H. pylori in Gastric Mucosa Using Advanced LNA Probes. Boneca IG, ed. *PLoS One*. 2015;10(4):e0125494. doi:10.1371/journal.pone.0125494

Fontenete S, Carvalho D, Guimarães N, et al. Application of locked nucleic acid-based probes in fluorescence in situ hybridization. *Appl Microbiol Biotechnol*. 2016;100(13):5897-5906. doi:10.1007/s00253-016-7429-4

Frickmann H, Zautner AE, Moter A, et al. Fluorescence *in situ* hybridization (FISH) in the microbiological diagnostic routine laboratory: a review. *Crit Rev Microbiol*. 2017;43(3):263-293. doi:10.3109/1040841X.2016.1169990

Fukuda K, Ogawa M, Taniguchi H, Saito M. Molecular Approaches to Studying Microbial Communities: Targeting the 16S Ribosomal RNA Gene. *J UOEH*. 2016;38(3):223-232. doi:10.7888/juoeh.38.223

Garini Y, Young IT, McNamara G. Spectral imaging: Principles and applications. *Cytom Part A*. 2006;69A(8):735-747. doi:10.1002/cyto.a.20311

Ge Z, Sheh A, Feng Y, et al. Helicobacter pylori-infected C57BL/6 mice with different gastrointestinal microbiota have contrasting gastric pathology, microbial and host immune responses. *Sci Rep*. 2018;8(1):8014. doi:10.1038/s41598-018-25927-2

Gerstein AS. *Molecular Biology Problem Solver Molecular Biology Problem Solver: A Laboratory Guide. Edited.*; 2001. www.Wiley.com. Accessed May 30, 2019.

Giesen U, Kleider W, Berding C, Geiger A, Orum H, Nielsen PE. A formula for thermal stability (Tm) prediction of PNA/DNA duplexes. *Nucleic Acids Res*. 1998;26(21):5004-5006. doi:10.1093/nar/26.21.5004

Giovannoni SJ, DeLong EF, Olsen GJ, Pace NR. Phylogenetic group-specific oligodeoxynucleotide probes for identification of single microbial cells. *J Bacteriol*. 1988;170(2):720-726. doi:10.1128/jb.170.2.720-726.1988

Gordon AM. Application of Fluorescence in situ Hybridization for Visualization and Quantification of Human Gastrointestinal Microbiota. 2015.

Guimarães N, Azevedo NF, Figueiredo C, Keevil CW, Vieira MJ. Development and application of a novel peptide nucleic acid probe for the specific detection of Helicobacter pylori in gastric biopsy specimens. *J Clin Microbiol*.

2007;45(9):3089-3094. doi:10.1128/JCM.00858-07

Guinane CM, Cotter PD. Role of the gut microbiota in health and chronic gastrointestinal disease: understanding a hidden metabolic organ. Therap Adv Gastroenterol. 2013;6(4):295-308. doi:10.1177/1756283X13482996

Hiraoka Y, Shimi T, Haraguchi T. Multispectral imaging fluorescence microscopy for living cells. Cell Struct Funct. doi: 10.1247/csf.27.367

Hogardt M, Trebesius K, Geiger AM, Hornef M, Rosenecker J, Heesemann J. Specific and rapid detection by fluorescent in situ hybridization of bacteria in clinical samples obtained from cystic fibrosis patients. *J Clin Microbiol*. 2000;38(2):818-825.

Hörmannsperger G, Schaubeck M, Haller D. Intestinal Microbiota in Animal Models of Inflammatory Diseases. 2015. doi:10.1093/ilar/ilv019

Hugenholtz F, de Vos WM. Mouse models for human intestinal microbiota research: a critical evaluation. *Cell Mol Life Sci*. 2018;75(1):149-160. doi:10.1007/s00018-017-2693-8

Hasegawa Y, Welch JLM, Valm AM, Rieken CW, Sogin ML, Borisy GG. Imaging marine bacteria with unique 16S rRNA V6 sequences by fluorescence in situ hybridization and spectral analysis. Geomicrobiol J. 2010;27(3):251-260. doi:10.1080/01490450903456806

Ikoma H, Heshmat B, Wetzstein G, Raskar R. Attenuation-corrected fluorescence spectra unmixing for spectroscopy and microscopy. Opt Express. 2014;22(16):19469. doi:10.1364/OE.22.019469

Ishaq S, Nunn L. Helicobacter pylori and gastric cancer: a state of the art review. Gastroenterol Hepatol from bed to bench. doi: 10.22037/ghfbb.v8iSupplement.653

James B. Pawlet. Handbook of Biological Confocal Microscopy. In: ; 2006. https://books.google.pt/books?hl=pt-PT&lr=&id=IKcPnaNPrhoC&oi=fnd&pg=PR5&dq=Handbook+of+biological+confocal+microscopy,+Springer+Science+%26+Business+Media.&ots=rbOlMs5huq&sig=5HaTPiDIpX1kHfm5Wm7lNUjxZ_4&redir_esc=y#v=onepage&q=Handbook%2520of%2520biological%25. Accessed March 16, 2019.

Jansen GJ, Mooibroek M, Idema J, Harmsen HJ, Welling GW, Degener JE. Rapid identification of bacteria in blood cultures by using fluorescently labeled oligonucleotide probes. *J Clin Microbiol*. 2000;38(2):814-817

John HA, Birnstiel ML, Jones KW. RNA-DNA Hybrids at the Cytological Level. *Nature*. 1969;223(5206):582-587. doi:10.1038/223582a0

Johnson I. The Molecular Probes Handbook. A Guide to Fluorescent Probes and Labeling Technologies. 2005.

Kempf VA, Trebesius K, Autenrieth IB. Fluorescent In situ hybridization allows rapid identification of microorganisms in blood cultures. *J Clin Microbiol*. 2000;38(2):830-838

Kienesberger S, Cox LM, Livanos A, et al. Gastric Helicobacter pylori Infection Affects Local and Distant Microbial Populations and Host Responses. *Cell Rep*. 2016;14(6):1395-1407. doi:10.1016/j.celrep.2016.01.017

Klappenbach JA, Dunbar JM, Schmidt TM. rRNA operon copy number reflects ecological strategies of bacteria. *Appl Environ Microbiol*. 2000;66(4):1328-1333

Kraft CH, Monstein H-J, Borch K, Tiveljung A, Jonasson J. Profiling of bacterial flora in gastric biopsies from patients with Helicobacter pylori-associated gastritis and histologically normal control individuals by temperature gradient gel electrophoresis and 16S rDNA sequence analysis. *J Med Microbiol*. 2000;49(9):817-822. doi:10.1099/0022-1317-49-9-817

Kraus B, Ziegler M, Wolff H. Linear fluorescence unmixing in cell biological research. *Mod Res Educ Top Microsc*. 2007:863-872.

Kubota K, Ohashi A, Imachi H, Harada H. Improved In Situ Hybridization Efficiency with Locked-Nucleic-Acid-Incorporated

DNA Probes. *Appl Environ Microbiol*. 2006;72(8):5311-5317. doi:10.1128/AEM.03039-05

Kusters JG, van Vliet AHM, Kuipers EJ. Pathogenesis of Helicobacter pylori infection. *Clin Microbiol Rev*. 2006;19(3):449-490. doi:10.1128/CMR.00054-05

Kwon H-S, Yang E-H, Yeon S-W, Kang B-H, Kim T-Y. Rapid identification of probiotic *Lactobacillus* species by multiplex PCR using species-specific primers based on the region extending from 16S rRNA through 23S rRNA. *FEMS Microbiol Lett*. 2004;239(2):267-275. doi:10.1016/j.femsle.2004.08.049

Lansford R, Bearman G, Fraser SE. Resolution of multiple green fluorescent protein color variants and dyes using two-photon microscopy and imaging spectroscopy. *J Biomed Opt*. 2001;6(3):311. doi:10.1117/1.1383780

Lay G. *Fluorochromes Brightness Index*.; 2009. https://www.biolegend.com/media_assets/support_resource/Fluorochrome_Brightness_Index.pdf. Accessed June 17, 2019.

Levsky JM, Singer RH. Fluorescence in situ hybridization: past, present and future. *J Cell Sci*. 2003;116(14):2833-2838. doi:10.1242/JCS.00633

Li X-X, Wong GL-H, To K-F, et al. Bacterial Microbiota Profiling in Gastritis without Helicobacter pylori Infection or Non-Steroidal Anti-Inflammatory Drug Use. Ahmed N, ed. *PLoS One*. 2009;4(11):e7985. doi:10.1371/journal.pone.0007985

Llobet-Brossa E, Rosselló-Mora R, Amann R. Microbial Community Composition of Wadden Sea Sediments as Revealed by Fluorescence In Situ Hybridization. *Appl Environ Microbiol*. 1998;64(7):2691-2696

Lücker S, Steger D, Urup Kjeldsen K, MacGregor BJ, Wagner M, Loy A. Supplementary Online Material (SOM) Improved 16S RRNA- Lofgren JL, Whary MT, Ge Z, et al. Lack of commensal flora in H. pylori-infected INS-GAS mice reduces gastritis and delays intraepithelial neoplasia. *Gastroenterology*. 2011;140(1):210. doi:10.1053/J.GASTRO.2010.09.048

Majlessi M, Nelson NC, Becker MM. Advantages of 2'-O-methyl oligoribonucleotide probes for detecting RNA targets. *Nucleic Acids Res*. 1998;26(9):2224-2229

Maldonado-Contreras A, Goldfarb KC, Godoy-Vitorino F, et al. Structure of the human gastric bacterial community in relation to Helicobacter pylori status. *ISME J*. 2011;5(4):574-579. doi:10.1038/ismej.2010.149

Margo CE, Bombardier T. The diagnostic value of fungal autofluorescence. *Surv Ophthalmol*. 1985;29(5):374-376. doi:10.1016/0039-6257(85)90114-6

Matthiesen SH, Hansen CM. Fast and Non-Toxic In Situ Hybridization without Blocking of Repetitive Sequences. Metze K, ed. *PLoS One*. 2012;7(7):e40675. doi:10.1371/journal.pone.0040675

Mendes L, Rocha R, Azevedo AS, et al. Novel strategy to detect and locate periodontal pathogens: The PNA-FISH technique. *Microbiol Res*. 2016;192:185-191. doi:10.1016/j.micres.2016.07.002

Morrison LE, Ramakrishnan R, Ruffalo TM, Wilber KA. Labeling Fluorescence In Situ Hybridization Probes for Genomic Targets. In: *Molecular Cytogenetics*. Vol 204. New Jersey: Humana Press; 2002:21-40. doi:10.1385/1-59259-300-3:21

Moter A, Göbel UB. Fluorescence in situ hybridization (FISH) for direct visualization of microorganisms. *J Microbiol Methods*. 2000;41(2):85-112

Muro MA. Probe Design, Production, and Applications. In: *Medical Biomethods Handbook*. Totowa, NJ: Humana Press; 2005:13-23. doi:10.1385/1-59259-870-6:013

Murphy DB, Piston DW, Shand SH, Davidson MW. Spectral Bleed - Through Artifacts in Confocal Microscopy. 2017;2:1-7.

Targeted Probe Set for Analysis of Sulfate-Reducing Bacteria by Fluorescence In Situ Hybridization. Vol 69.; 2007.

http://www.microbial-ecology.net/probebase/. Accessed May 21, 2019.

Nardone G, Compare D. The human gastric microbiota: Is it time to rethink the pathogenesis of stomach diseases? *United Eur Gastroenterol J*. 2015;3(3):255-260. doi:10.1177/2050640614566846

Nguyen TLA, Vieira-Silva S, Liston A, Raes J. How informative is the mouse for human gut microbiota research? Dis Model Mech. 2015;8(1):1-16. doi:10.1242/dmm.017400

Nielsen PE, Egholm M, Berg RH, Buchardt O. Sequence-selective recognition of DNA by strand displacement with a thymine-substituted polyamide. *Science*. 1991;254(5037):1497-1500

Nordentoft S, Christensen H, Wegener HC. Evaluation of a fluorescence-labelled oligonucleotide probe targeting 23S rRNA for in situ detection of Salmonella serovars in paraffin-embedded tissue sections and their rapid identification in bacterial smears. *J Clin Microbiol*. 1997;35(10):2642-2648

Noto JM, Peek RM, Jr. The gastric microbiome, its interaction with Helicobacter pylori, and its potential role in the progression to stomach cancer. PLoS Pathog. 2017;13(10):e1006573. doi:10.1371/journal.ppat.1006573

Pardue ML, Gall JG. MOLECULAR HYBRIDIZATION OF RADIOACTIVE DNA TO THE DNA OF CYTOLOGICAL PREPARATIONS. *Proc Natl Acad Sci*. 1969;64(2):600-604. doi:10.1073/pnas.64.2.600

Pautke C, Tischer T, Vogt S, et al. New advances in fluorochrome sequential labelling of teeth using seven different fluorochromes and spectral image analysis. *J Anat*. 2007;210(1):117-121. doi:10.1111/j.1469-7580.2006.00660.x

Perlman RL. Mouse models of human disease: An evolutionary perspective. *Evol Med public Heal*. 2016;2016(1):170-176. doi:10.1093/emph/eow014

Petersen M, Wengel J. LNA: a versatile tool for therapeutics and genomics. *Trends Biotechnol*. 2003;21(2):74-81. doi:10.1016/S0167-7799(02)00038-0

Petra CV, Rus A, Dumitraşcu DL. Gastric microbiota: tracing the culprit. *Clujul Med*. 2017;90(4):369-376. doi:10.15386/cjmed-854

Properties of ATTO-Dyes. https://www.atto-tec.com/fileadmin/user_upload/Katalog_Flyer_Support/Dye_Properties_01.pdf. Accessed June 19, 2019.

Rieken CW, Dewhirst FE, Valm AM, et al. Systems-level analysis of microbial community organization through combinatorial labeling and spectral imaging. *Proc Natl Acad Sci*. 2011;108(10):4152-4157. doi:10.1073/pnas.1101134108

Rocha R, Almeida C, Azevedo NF. Influence of the fixation/permeabilization step on peptide nucleic acid fluorescence in situ hybridization (PNA-FISH) for the detection of bacteria. Zhou Z, ed. *PLoS One*. 2018;13(5):e0196522. doi:10.1371/journal.pone.0196522

Roos S, Engstrand L, Jonsson H. Lactobacillus gastricus sp. nov., Lactobacillus antri sp. nov., Lactobacillus kalixensis sp. nov. and Lactobacillus ultunensis sp. nov., isolated from human stomach mucosa. *Int J Syst Evol Microbiol*. 2005;55(1):77-82. doi:10.1099/ijs.0.63083-0

Rudkin GT, Stollar BD. High resolution detection of DNA-RNA hybrids in situ by indirect immunofluorescence. *Nature*. 1977;265(5593):472-473

Ruiz SI, Zumbrun EE, Nalca A. *Animal Models of Human Viral Diseases*.; 2017. doi:10.1016/B978-0-12-809468-6.00033-4

Savage DC. Microbial Ecology of the Gastrointestinal Tract. *Annu Rev Microbiol*. 1977;31(1):107-133. doi:10.1146/annurev.mi.31.100177.000543

Silahtaroglu A, Pfundheller H, Koshkin A, Tommerup N, Kauppinen S. LNA-modified oligonucleotides are highly efficient as FISH probes. *Cytogenet Genome Res*. 2004;107(1-2):32-37. doi:10.1159/000079569

Silverman AP, Kool ET. Oligonucleotide Probes for RNA-Targeted Fluorescence In Situ Hybridization. *Adv Clin Chem*.

2007;43:79-115. doi:10.1016/S0065-2423(06)43003-1

Stark CA, Adamsson I, Edlund C, et al. Effects of omeprazole and amoxycillin on the human oral and gastrointestinal microflora in patients with *Helicobacter pylori* infection. *J Antimicrob Chemother*. 1996;38(6):927-939. doi:10.1093/jac/38.6.927

Stender H, Fiandaca M, Hyldig-Nielsen JJ, Coull J. PNA for rapid microbiology. *J Microbiol Methods*. 2002;48(1):1-17

Takao K, Miyakawa T. Genomic responses in mouse models greatly mimic human inflammatory diseases. *Proc Natl Acad Sci U S A*. 2015;112(4):1167-1172. doi:10.1073/pnas.1401965111

Testerman TL, Morris J. Beyond the stomach: an updated view of Helicobacter pylori pathogenesis, diagnosis, and treatment. World J *Gastroenterol*. 2014;20(36):12781-12808. doi:10.3748/wjg.v20.i36.12781

Thursby E, Juge N. Introduction to the human gut microbiota. *Biochem J*. 2017;474(11):1823-1836. doi:10.1042/BCJ20160510

Treuting PM, Dintzis SM. *Comparative Anatomy and Histology : A Mouse and Human Atlas*. Academic; 2012.

Tropini C, Earle KA, Huang KC, Sonnenburg JL. The Gut Microbiome: Connecting Spatial Organization to Function. *Cell Host Microbe*. 2017;21(4):433-442. doi:10.1016/j.chom.2017.03.010

Tsay F-W, Hsu P-I. H. pylori infection and extra-gastroduodenal diseases. *J Biomed Sci*. 2018;25(1):65. doi:10.1186/s12929-018-0469-6

Tsurui H, Nishimura H, Hattori S, Hirose S, Okumura K, Shirai T. Seven-color Fluorescence Imaging of Tissue Samples Based on Fourier Spectroscopy and Singular Value Decomposition. *J Histochem Cytochem*. 2000;48(5):653-662. doi:10.1177/002215540004800509

Ursell LK, Metcalf JL, Parfrey LW, Knight R. Defining the human microbiome. *Nutr Rev*. 2012;70:S38-S44. doi:10.1111/j.1753-4887.2012.00493.x

Valm AM, Mark Welch JL, Borisy GG. CLASI-FISH: Principles of combinatorial labeling and spectral imaging. *Syst Appl Microbiol*. 2012;35(8):496-502. doi:10.1016/J.SYAPM.2012.03.004

Valm AM, Mark Welch JL, Borisy GG. CLASI-FISH: Principles of combinatorial labeling and spectral imaging. *Syst Appl Microbiol*. 2012;35(8):496-502. doi:10.1016/j.syapm.2012.03.004

Valm AM, Oldenbourg R, Borisy GG. Multiplexed Spectral Imaging of 120 Different Fluorescent Labels. Brody JP, ed. *PLoS One*. 2016;11(7):e0158495. doi:10.1371/journal.pone.0158495

Valm AM, Oldenbourg R, Borisy GG. Multiplexed spectral imaging of 120 different fluorescent labels. *PLoS One*. 2016;11(7):1-17. doi:10.1371/journal.pone.0158495

Vartoukian SR, Palmer RM, Wade WG. Strategies for culture of 'unculturable' bacteria. *FEMS Microbiol Lett*. 2010;309(1):no-no. doi:10.1111/j.1574-6968.2010.02000.x

Velin D, Michetti P. Immunology of Helicobacter pylori infection. *Digestion*. 2006;73(2-3):116-123. doi:10.1159/000094043

Vogt S, Kolk A, Haczek C, et al. New advances in fluorochrome sequential labelling of teeth using seven different fluorochromes and spectral image analysis. *J Anat*. 2006;210(1):117-121. doi:10.1111/j.1469-7580.2006.00660.x

Wagner M, Amann R. *Molecular Technique for Determining Microbial Community Structures in Activated Sludge*.; 2001. https://books.google.pt/books?id=prWXOYIo63QC&pg=RA2-PP13&lpg=RA2-PP13&dq=molecular+technique+for+determining+microbial+community+structures+in+activated+sludge&source=bl&ots=HsDOT1YH-D&sig=ACfU3U2JrSvcBDR1-Yv0_iL_vcUsI1-EvQ&hl=pt-PT&sa=X&ved=2ahUKEwjH4If. Accessed June 14, 2019.

Wahlestedt C, Salmi P, Good L, et al. Potent and nontoxic antisense oligonucleotides containing locked nucleic acids. *Proc*

Natl Acad Sci U S A. 2000;97(10):5633-5638. doi:10.1073/PNAS.97.10.5633

Wang L-L, Yu X-J, Zhan S-H, Jia S-J, Tian Z-B, Dong Q-J. Participation of microbiota in the development of gastric cancer. *World J Gastroenterol*. 2014;20(17):4948-4952. doi:10.3748/wjg.v20.i17.4948

Wessendorf MW, Brelje TC. Which fluorophore is brightest? A comparison of the staining obtained using fluorescein, tetramethylrhodamine, lissamine rhodamine, Texas red, and cyanine 3.18. Histochemistry. 1992;98(2):81-85

Whary MT, Muthupalani S, Ge Z, et al. Helminth co-infection in Helicobacter pylori infected INS-GAS mice attenuates gastric premalignant lesions of epithelial dysplasia and glandular atrophy and preserves colonization resistance of the stomach to lower bowel microbiota. Microbes Infect. 2014;16(4):345-355. doi:10.1016/J.MICINF.2014.01.005

Woese CR. Bacterial evolution. Microbiol Rev. 1987;51(2):221-271

Wu WM, Yang YS, Peng LH. Microbiota in the stomach: New insights. J Dig Dis. 2014;15(2):54-61. doi:10.1111/1751-2980.12116

Wu Q, Li Y, Wang M, Pan XP, Tang YF. Fluorescence in situ hybridization rapidly detects three different pathogenic bacteria in urinary tract infection samples. *J Microbiol Methods*. 2010;83(2):175-178. doi:10.1016/j.mimet.2010.08.015

Yang I, Nell S, Suerbaum S. Survival in hostile territory: the microbiota of the stomach. *FEMS Microbiol Rev*. 2013;37(5):736-761. doi:10.1111/1574-6976.12027

Yaroslavsky AI, Smolina IV. Fluorescence Imaging of Single-Copy DNA Sequences within the Human Genome Using PNA-Directed Padlock Probe Assembly. *Chem Biol*. 2013;20(3):445-453. doi:10.1016/j.chembiol.2013.02.012

Yilmaz LS, Noguera DR. Mechanistic approach to the problem of hybridization efficiency in fluorescent in situ hybridization. *Appl Environ Microbiol*. 2004;70(12):7126-7139. doi:10.1128/AEM.70.12.7126-7139.2004

Yilmaz LS, Noguera DR. Mechanistic Approach to the Problem of Hybridization Efficiency in Fluorescent In Situ Hybridization. *Appl Environ Microbiol*. 2004;70(12):7126-7139. doi:10.1128/AEM.70.12.7126-7139.2004

Younger ST, Corey DR. The puzzle of RNAs that target gene promoters. *Chembiochem*. 2009;10(7):1135-1139. doi:10.1002/cbic.200900015

Zimmermann T, Rietdorf J, Pepperkok R. Spectral imaging and its applications in live cell microscopy. *FEBS Lett*. 2003;546(1):87

Appendix 1. Selection of mouse gastric bacterial species

4 gastric samples of C57BL/6 mices were sequenced by IPATIMUP/i3S team researcher. The results suggested that the gastric microbiota consists of *Lactobacillus* sp, including *Lactobacillus murins*, Clostridiales, *Bacteroides* sp., *Muribaculum intestinale* and *Faecalibaculum rodentium*.

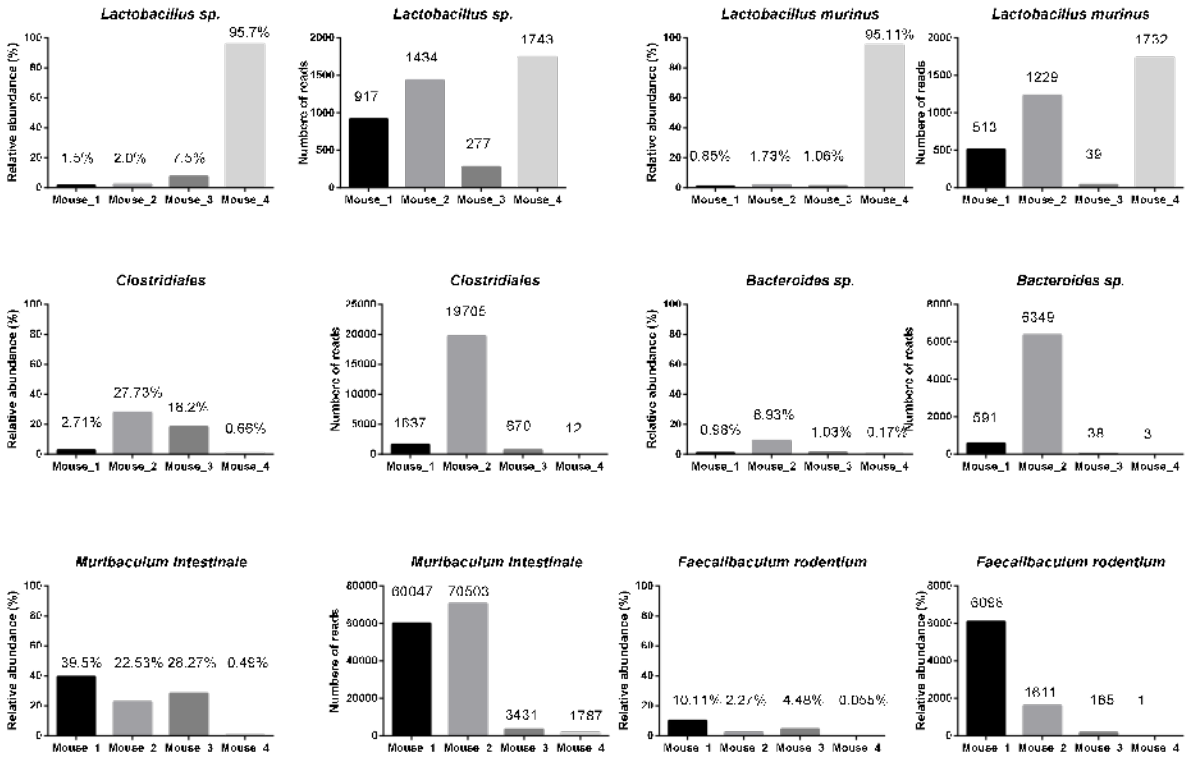

Figure A1. Gastric samples of 4 C57BL76 mices sequenced. Mouse gastric microbiota is constituted by *Lactobacillus* sp., Clostridiales, *Bacteroides* sp., *Muribaculum intestinale* and *Faecalibaculum rodentium*. Made by Rui Ferreira from IPMATIMUP/i3S.

Appendix 2. Intensity Fluorescence Quantification

There are a number of different ways to get intensity information from images using the base package of ImageJ (no plugins required).

The main steps to quantify the intensity fluorescence are schematized in Figure A2. Firstly, duplicate the original image and then it was defined a specific threshold, selecting B&W and Dark Background and adjusting the value (B. Figure A2); in order to minimize the variations, it was necessary to use a method that reduces the difference for each measurement, so we use automatically. The binary image was processed assuming black cells on a white background. Watershed segmentation (C, Figure A2) was selected to separate nearby cells allowing an automatically separations or cutting apart cells that touch. Redirecting to the duplicated channel image, the option analyze particles (D. Figure A2) was selected and the same parameters were defined for several images: Size: 0-infinity; Circularity: 0.00-1.00. Then, set measurement was selected and the following parameters were defined after the analysis of several images: Area, Standard deviation, Mean gray value and Display label.

Subsequently, the results are shown in a new window (E. Figure A2), ROI manager. In addition, the more succinct results as the mean of fluorescence intensity, %Area, Average size appear in summary. Then, these results are saved an excel document with these parameters of all the images placed in the folder.

1) Open image;
2) Duplicate the image; we should always duplicate the images for do not change the original images.

   Image – Duplicate;
3) Smooth to standardize the color of each pixel of the images.

   Process – Smooth
4) Apply a filter if the image is not clear.

   Process – Filters;
5) Apply an automatic to all images.

   Threshold Image – Adjust – Threshold – Auto – Apply
6) Process – Binary – Watershed
7) Analyze – Set measurements and check off the box next to “Limit to Threshold”
8) Analyze – Analyze Particles
9) Results – Summarize

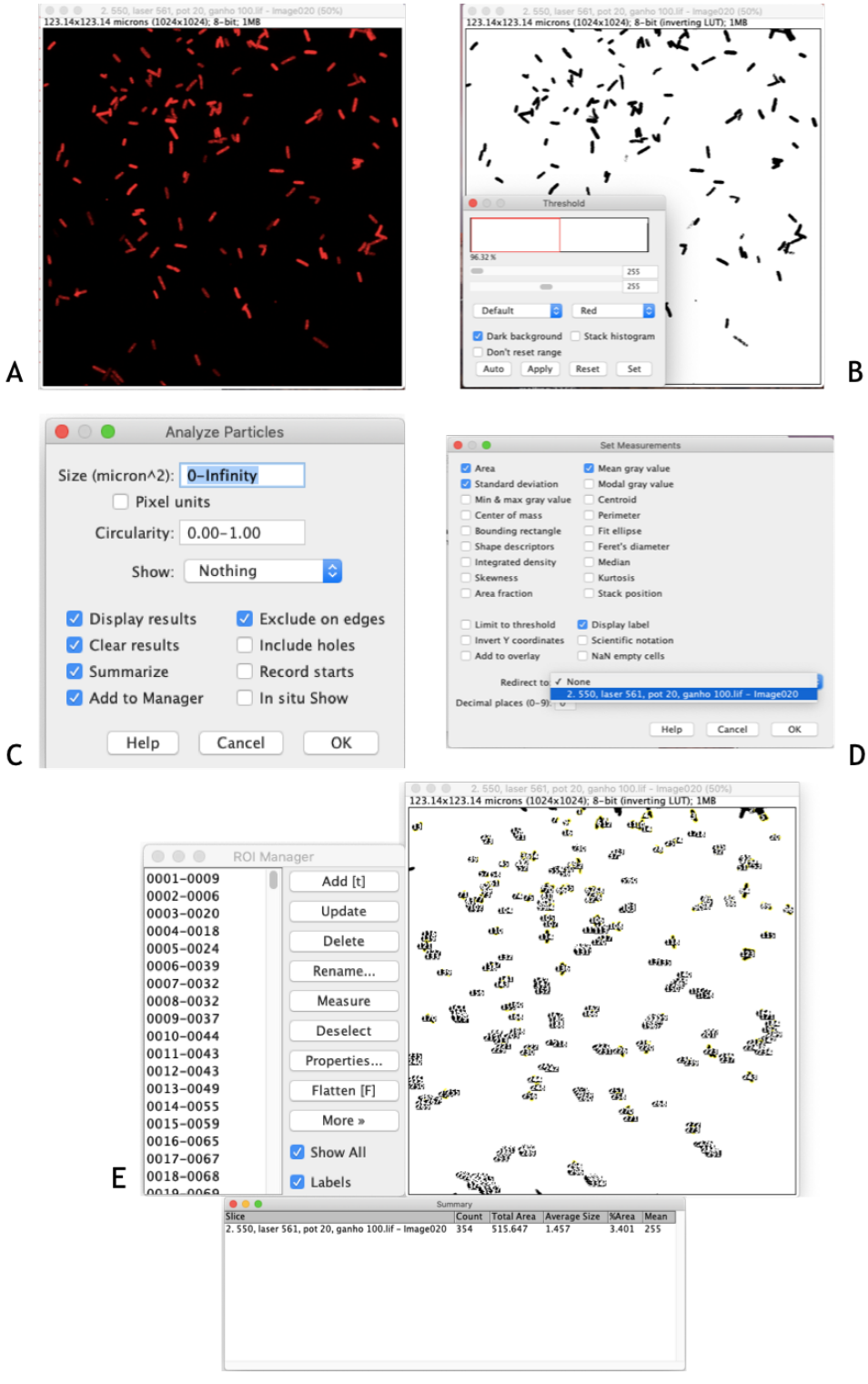

Figure A2. **Fluorescence intensity measurement with Fiji software.** A. Open Image; B. Adjust threshold; C. Watershed; D. Analyze Particles; E. Save data from ROI manager.

Appendix 3. Linear Unmixing

Once a spectral image is acquired, the challenge then become one of assignment. Each of the hundreds of thousands of spectra recorded ate every pixel in an image must be identified as belonging to a particular fluorochrome.

Linear unmixing is a computational method for fluorochrome assignment that is used in confocal microscope for spectral images. Thus, the confocal algorithm was applied to generate multichannel images (Figure A3, Figure A5, Figure A4, Figure A6).

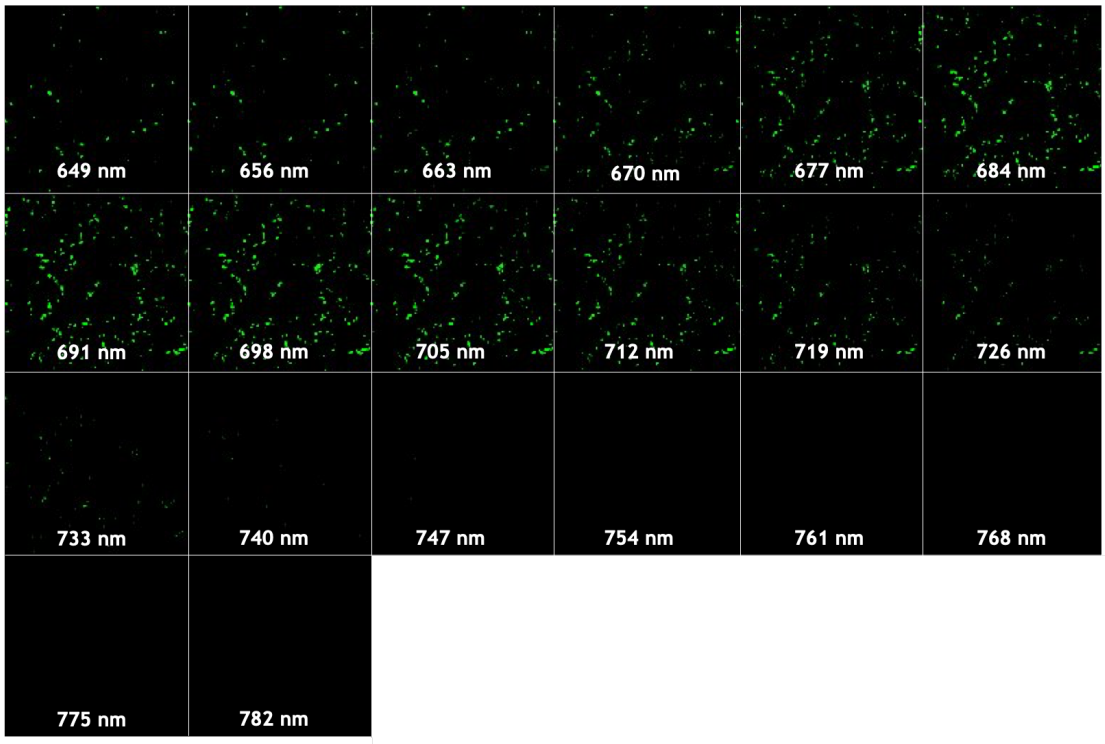

Figure A3. A 20-channel spectral image of a mixture of *Faecalibaculum rodentum* coupled with ATTO 655 and *Mutibaculum intestinale* coupled with ATTO 633. In each channel 7 nm of visible wavelength emission was recorded from 649 nm to 782 nm.

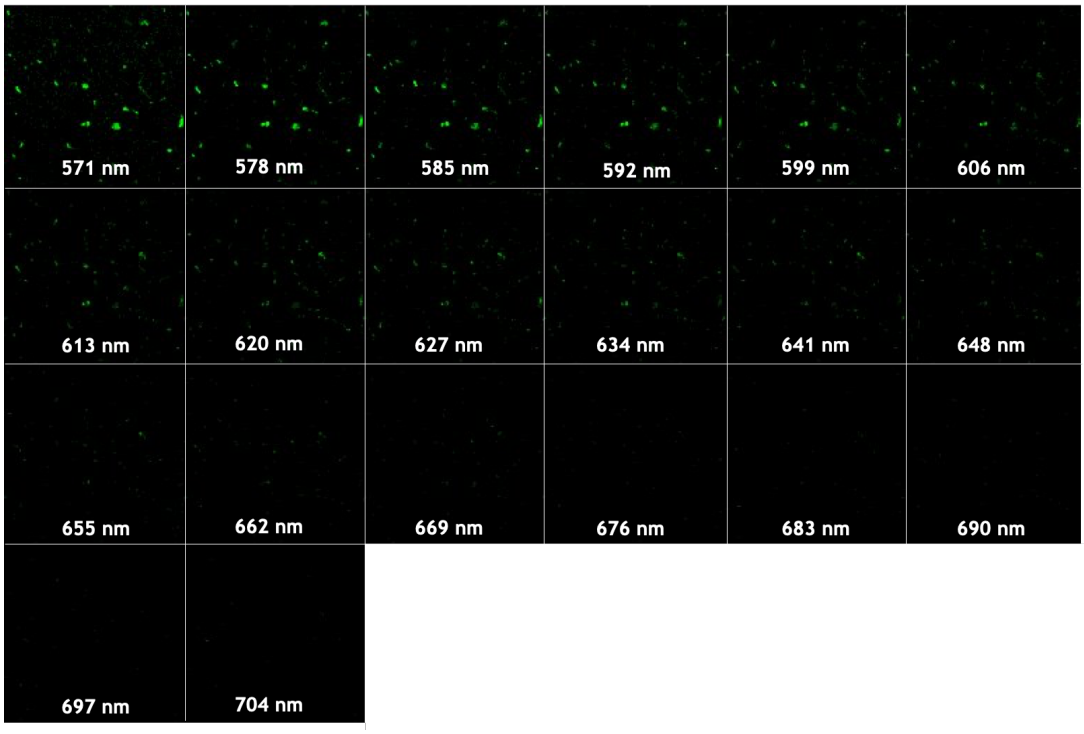

Figure A5. A 20-channel spectral image of a mixture of *Bacteroides dorei* coupled with Alexa Fluor 594 and *Helicobacter pylori* coupled with ATTO 550. In each channel 7 nm of visible wavelength emission was recorded from 571 nm to 704 nm.

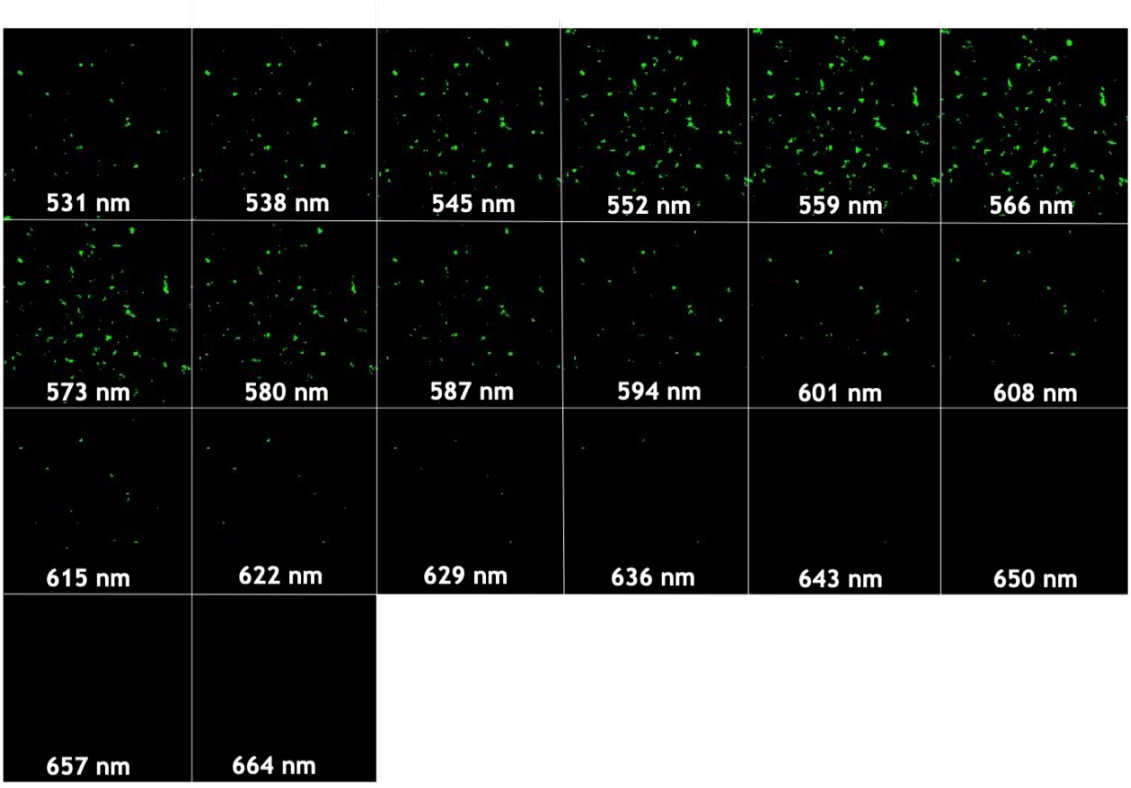

Figure A4. A 20-channel spectral image of a mixture of *Lactobacillus paracasei* coupled with ATTO 532 and *Clostridioides mangenotii* coupled with Alexa Fluor 514. In each channel 7 nm of visible wavelength emission was recorded from 531 nm to 664 nm.

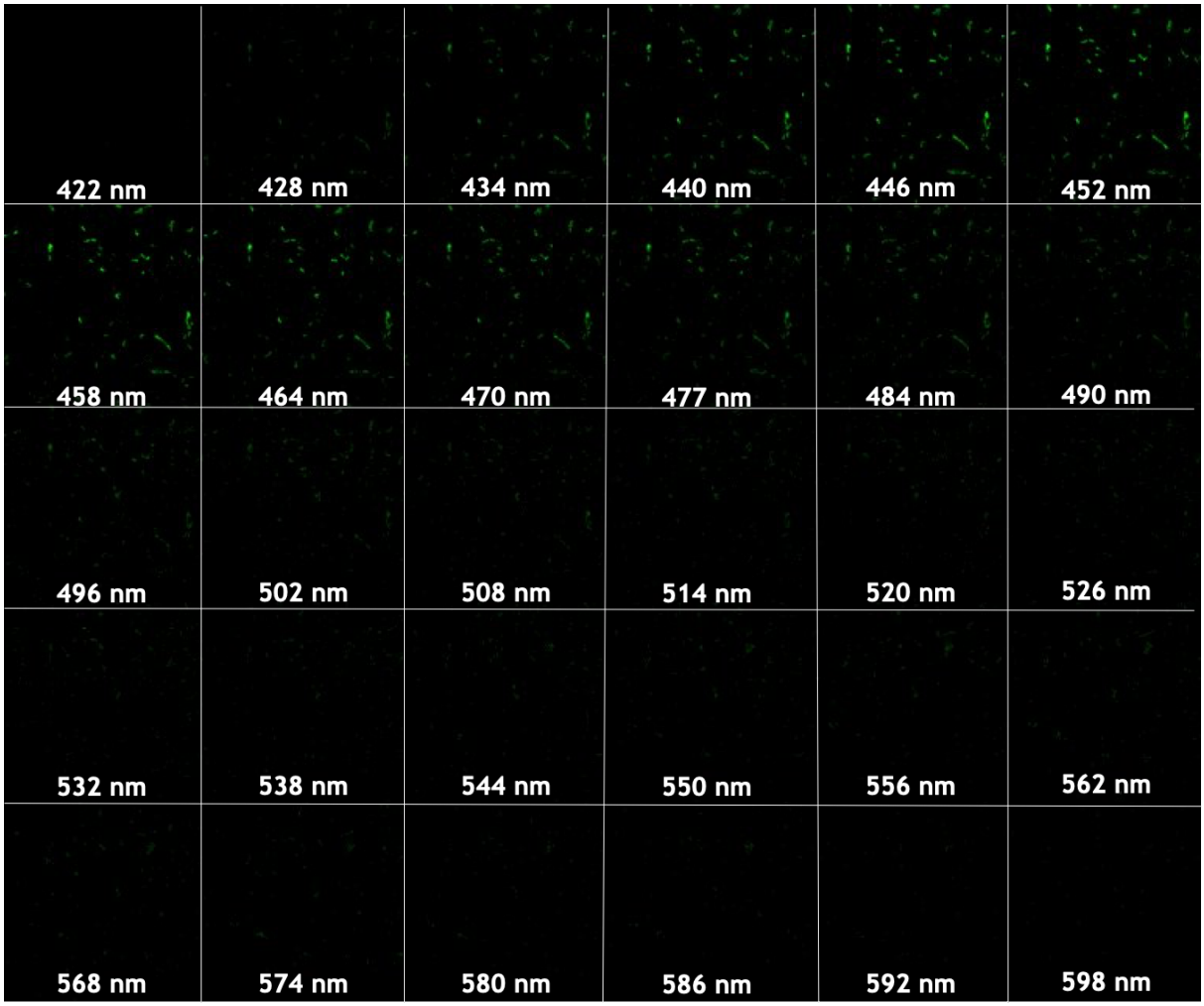

Figure A6. A 30-channel spectral image of *Citrobacter freundii* coupled with Alexa Fluor 405. In each channel 6 nm of visible wavelength emission was recorded from 422 nm to 598 nm.

Appendix 4. Image Analysis

The four separate spectral image stacks were trimmed so that wavelength channels in which negligible light intensity was recorded were discarded. The four separate spectral image stacks were then concatenated to create a single excitation / emission spectral image data set.

Each channel is kept separate from the other and can be turned on or off using Channels Tools (Figure A7.C). For viewing the image as a composite of all the different channels with different colors we made make composite. We can change the colors by applying lookup tables (Figure A7.B). Then, it is applied Stack to RGB to combine singles images into one single RGB image (Figure A7.D). Finally, Z Project (Figure A7.E) is applied for analyzing a stack by applying different projection methods to the pixels within the stack. The projection type choose for this images were sum slices that creates a real image that is sum of the slices in the stack.

After the linear unmixing algorithm applied (Appendix 3):

1) Open each sequential analysis in Fiji software;

   Sequential Analysis 4 contains ATTO 655 and ATTO 633;

   Sequential Analysis 3 contains Alexa Fluor 594 and ATTO 550;

   Sequential Analysis 2 contains ATTO 532 and Alexa Fluor 514;

   Sequential Analysis 1 contains Alexa Fluor 405.

2) In order to split apart the separate channels:

   Image - Color - Split channel

   -Attribution color to each channel (lookup tables – select color);

3) Save each image;

4) Open each image in order;

5) Then, concatenate allows to add the slice of one attack at the end of another:

   Image – Tools – Concatenate;

6) To change the way the images is displayed:

   Image - Color – Channel tools – Make composite

   -Attribution of colors to each fluorochrome (lookup tables – select color);

7) Image - Color – Stack to RGB;

8) To create a maximum projection view:

Image – Stacks – Z project.

9) To add a scale bar:

Analyze – Tools – Scale Bar

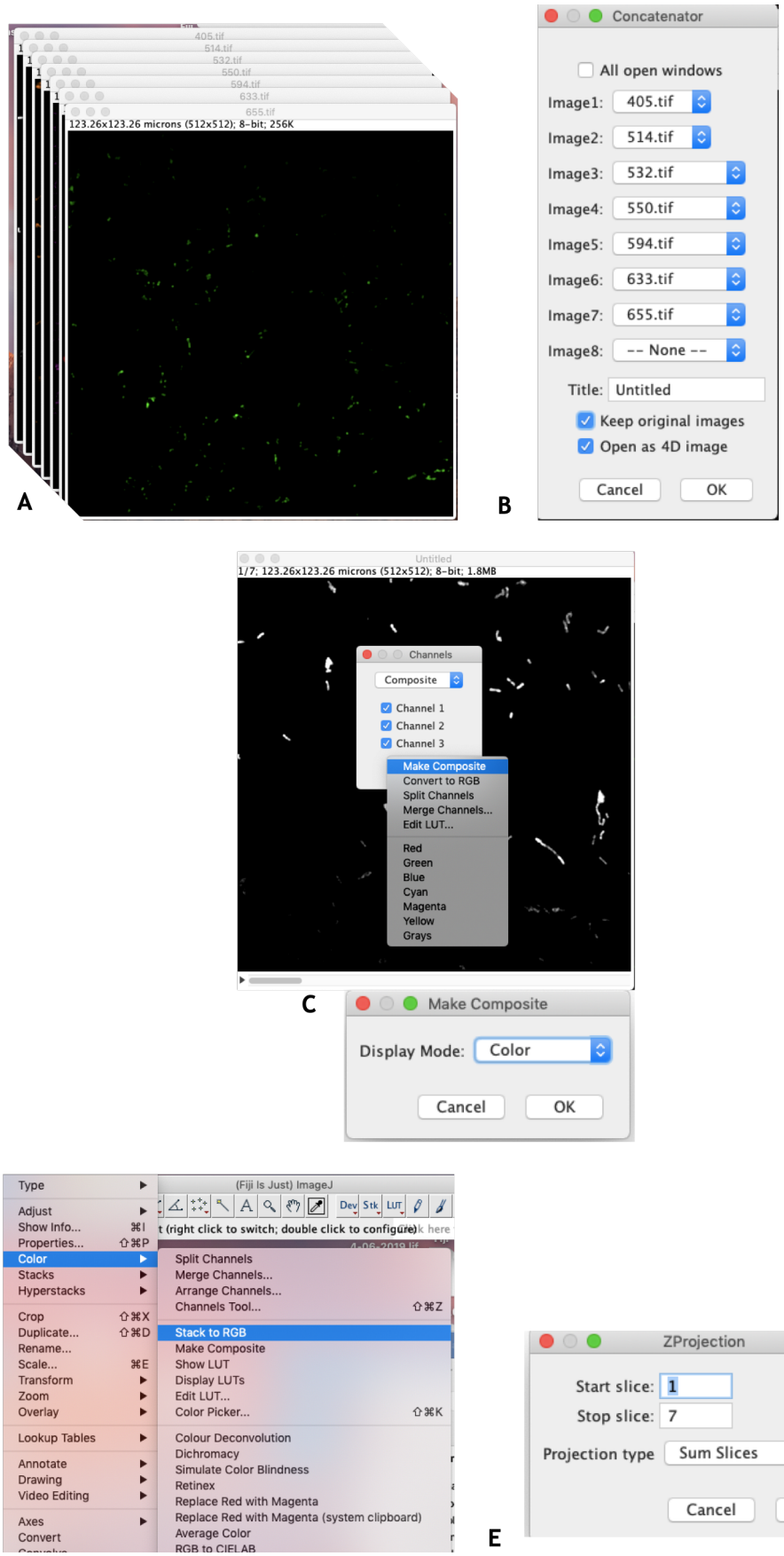

Figure A7. **Image analysis with Fiji software**. A. Open Images sequentially; B. Spectral images acquired were concatenate; C.Atributtion of color of each channel; D.Stacks to RGB; E. Z-Project

Appendix 5. Absorption and Emission Spectra of Fluorochromes

In this appendix are shown the spectral characteristics of each fluorochrome. These fluorochromes have distinct absorption and emission profiles, Table A1.

Table A1. Absorption and Emission Spectra of Fluorochromes: Alexa Fluor 405, Alexa Fluor 488, Alexa Fluor 514, ATTO 532, ATTO 550, Alexa Fluor594, ATTO 633 and ATTO 655.

Fluorochrome	Absorption	Emission
Alexa Fluor 405	401 nm	421 nm
Alexa Fluor 488	495 nm	519 nm
Alexa Fluor 514	517 nm	542 nm
ATTO 532	532 nm (515-545 nm)	553 nm
ATTO 550	554 nm (540 - 565 nm)	576 nm
Alexa Fluor 594	590 nm	617 nm
ATTO 633	629 nm (610-645 nm)	657 nm
ATTO 655	655 nm (640-660 nm)	680 nm